

# 南阿尔金尤努斯萨依高压花岗质片麻岩原岩 的形成时代与地球化学特征:对南阿尔金 陆壳深俯冲板片属性的进一步限定

PAK Sang Wan, 马拓, 盖永升, 康磊, 王超, 廖小莹, 刘良\*

(西北大学地质学系, 大陆动力学国家重点实验室, 陕西 西安 710069)

**摘要:**南阿尔金尤努斯萨依地区出露的高压花岗质片麻岩的  $\text{SiO}_2 = 71.01\% \sim 75.07\%$ ,  $\text{Al}_2\text{O}_3 = 12.31\% \sim 14.21\%$ , 全碱  $\text{Na}_2\text{O} + \text{K}_2\text{O} = 7.44\% \sim 8.37\%$ ,  $\text{MgO} = 0.26\% \sim 0.60\%$ ,  $^{\text{T}}\text{FeO} = 1.75\% \sim 2.62\%$ ,  $\text{CaO} = 0.95\% \sim 1.70\%$ , 具有高硅、高铝、高碱性的特征, 属于钙碱性过铝质花岗质岩石。其稀土总量为  $131.15 \times 10^{-6} \sim 234.34 \times 10^{-6}$ , 相对富集 Rb、Th、La 等大离子亲石元素而亏损 Ba、Ta、Nb、Sr、Ti,  $\sum_{\text{LREE}} / \sum_{\text{HREE}} = 5.07 \sim 7.67$ ,  $(\text{La}/\text{Yb})_{\text{N}} = 4.82 \sim 9.58$ , 具有强烈的 Eu 亏损 ( $\delta_{\text{Eu}} = 0.42 \sim 0.63$ ), 显示出 S 型花岗岩的特征。岩石 Sr/Ba 值 (0.11~0.15) 较低,  $\text{CaO}/\text{Na}_2\text{O} = 0.44 \sim 0.75 > 0.3$ , 显示原岩可能为陆壳沉积的杂砂质岩石。LA-ICP-MS 锆石 U-Pb 定年表明该花岗质高压岩石原岩的形成时代约为 900 Ma, 指示其所代表的构造岩浆事件可能与阿尔金及其周缘广泛报道的新元古代 Rodinia 超大陆汇聚的地质事件相关, 并进一步限定其侵入的阿尔金杂岩的形成时代主体应为早新元古代。该高压花岗质片麻岩原岩的形成时代 (~900 Ma) 远大于其发生高压变质的时代 (~500 Ma), 表明其原岩就位于地壳约 400 Ma 之后才发生俯冲遭受高压变质作用。显然, 该高压岩石的形成是陆壳俯冲作用的产物, 为进一步限定南阿尔金早古生代陆壳俯冲-深俯冲作用提供了新的依据。

**关键词:** 高压花岗质片麻岩; 原岩的形成时代; 原岩的地球化学; 新元古代; 南阿尔金

中图分类号: P588.347

文献标志码: A

文章编号: 1009-6248(2019)04-0076-22

## Geochronology and Geochemical Characteristics of the Protolith Rock of Younusisayi High Pressure Granitic Gneiss: a Further Study on the Properties of Continental Crust Subduction Plate in South Altyn Tagh

PAK Sang Wan, MA Tuo, GAI Yongsheng, KANG Lei, WANG Chao, LIAO Xiaoying, LIU Liang

(State Key Laboratory of Continental Dynamics, Department of Geology, Northwest University, Xi'an 710069, Shaanxi, China)

**Abstract:** The major elements of granite gneiss exhibit the following geochemical characteristics:  $\text{SiO}_2 = 71.01\% \sim 75.07\%$ ,  $\text{Al}_2\text{O}_3 = 12.31\% \sim 14.21\%$ ,  $\text{Na}_2\text{O} + \text{K}_2\text{O} = 7.44\% \sim 8.37\%$ ,  $\text{MgO} = 0.26\% \sim 0.60\%$ ,  $^{\text{T}}\text{FeO} = 1.75\% \sim 2.62\%$ , and  $\text{CaO} = 0.95\% \sim 1.70\%$ , which reveals a typical

收稿日期: 2019-03-08; 修回日期: 2019-05-21

基金项目: 国家自然科学基金重点基金(41430209), 国家重点基础研究发展计划项目(2015CB856103), 国家自然科学基金群体和面上基金(41421002、41602052、41672187), 西北大学大陆动力学国家重点实验室自主研究重点课题联合资助

作者简介: PAK Sang Wan(1989-), 男, 硕士研究生, 矿物岩石学方向。E-mail: flyingwing44@icloud.com

\* 通讯作者: 刘良(1956-), 男, 教授, 博士生导师, 从事矿物学、岩石学研究。E-mail: liuliang@nwu.edu.cn

calc-alkali peraluminous granitic rock series. The granitic gneisses are simultaneously characterized by relative enrichment in Rb, Th, K, La and depletion in Ba, Ta, Nb, Sr, Ti, their  $\sum_{\text{REE}}$  values range from  $131.15 \times 10^{-6}$  to  $234.34 \times 10^{-6}$ ,  $\sum_{\text{LREE}}/\sum_{\text{HREE}}$  ratios are  $5.07 \sim 7.67$ ,  $(\text{La}/\text{Yb})_{\text{N}}$  ratios vary from 4.82 to 9.58, and  $\delta_{\text{Eu}}$  value are  $0.42 \sim 0.63$ , showing the element distribution of collision-induced granite. Meanwhile, the geochemical results also show that the source rock of the gneiss may be mixed sand rock deposited by continental crust with  $\text{Sr}/\text{Ba} = 0.11 \sim 0.15$  and  $\text{CaO}/\text{Na}_2\text{O} = 0.44 \sim 0.75 > 0.3$ . LA-ICP-MS zircon U-Pb isotopic dating has acquired a Neoproterozoic age of  $899.7 \pm 4.0 \text{Ma}$ . Based on geochemistry and chronology research, it is rationally suggested that Younusiisayi granitic was formed in a syn-collision tectonic setting as the result of the partial melting of upper crust sandy rocks, as the response of Rodinia supercontinent aggregation event in the south. Meanwhile, this granite gneiss further indicated that the formation time of whole Altyn complex rocks should be Early Neoproterozoic. Moreover, a metamorphic age of  $\sim 500 \text{Ma}$  has been obtained, which is much younger than the protolith age, and indicates that the protolith rock of this granitic gneiss was intruded and located in the continental crust for about  $\sim 400 \text{Ma}$  before subduction and high-pressure metamorphism. Thus, the granitic gneiss is obviously the product of continental subduction, which produces new evidence for further defining the subduction-deep subduction of the continental crust during Paleozoic of south Altyn Tagh.

**Keywords:** high pressure granitic gneiss; age of protolith; geochemistry; Neoproterozoic; South Altyn Tagh

高压-超高压带记录了地壳物质从俯冲到折返的动力学过程,被认为是板块俯冲-碰撞作用的产物,是古板块汇聚边界及大洋俯冲与大陆碰撞的重要标志(CHOPIN, 1984; SIMTH, 1988; ERNST, 1995, 2001; MARUYAMA et al., 1996; LIOU et al., 1998, 2009a; ZHENG, 2003, 2012)。目前,地质学者已在全球发现了 20 余条超高压变质带,并根据岩石组合、产状及变质作用特征将其划分为太平洋型(大洋型)和阿尔卑斯型(大陆型)2 种基本类型(ERNST et al., 1995; MARUYAMA et al., 1996; ERNST, 1988, 2001; LIOU et al., 2009b)。此外,也存在少数同时保留了洋壳深俯冲和陆壳深俯冲物质的特殊变质带。例如,柴北缘高压/超高压变质带(SONG et al., 2005; ZHANG et al., 2008a)。其中,太平洋型超高压带形成于大洋板块的深俯冲,主要由蛇绿岩套、岛弧火山岩序列、远洋硅质岩及灰岩组成的混杂岩及少量蓝片岩和榴辉岩组成(LIOU et al., 2009a, 2009b; SONG et al., 2014)。其中的 HP-UHP 榴辉岩峰期变质温度通常小于  $600^\circ\text{C}$ (REINECKE, 1991; LU et al., 2008; ERDMAN, 2014),其原岩均具有 MORB 等大洋玄武岩属性,且原岩形成时代与峰期变质时代之间不超过一个威尔逊旋回( $\sim 200 \text{Ma}$ )。例如,西南天

山,西阿尔卑斯 Zermatt-Saas 造山带(RUBATTO et al., 1998; ZHANG et al., 2007, 2008a)。阿尔卑斯型超高压带形成于陆壳的深俯冲,主要组成岩性包括花岗岩片麻岩、长英质和泥质副片麻岩、大理岩及少量呈透镜状或夹层状产于其中的榴辉岩、石榴子石橄榄岩、硬玉石英岩等。带中 HP-UHP 榴辉岩的峰期变质温度通常较高,且原岩类型比较复杂,既包括具有板内玄武岩和大陆溢流玄武岩等陆壳属性的榴辉岩,也包括先前就位的洋壳物质,即原岩形成时代与峰期变质时代相差大于一个威尔逊旋回。例如,中国大别-苏鲁造山带、北秦岭造山带、阿尔金造山带以及哈萨克斯坦 Kokchetav 地块等(ZHENG et al., 2006; LIU et al., 2009; LIOU et al., 2009a; 陈丹玲等, 2011)。因此,确定高压变质岩带的基本类型是高压-超高压变质岩带中各项研究工作的基础,亦是进一步深入理解高压岩石构造演化的前提。通过对高压变质岩石系统的地球化学工作,并结合区域内的岩石组合特征,是识别高压-超高压变质岩带洋/陆属性的有效途径。

南阿尔金是中国西部重要的高压-超高压变质岩带之一。先期研究已确定高压-超高压岩石主要分布在江孜勒萨依、英格丽萨依、淡水泉地区和木纳布拉克 4 个地区(图 1c);岩石类型包括榴辉岩、石

榴石石榴岩、石榴子石辉石岩、花岗质片麻岩和泥质片麻岩等;对其地质特征、岩石组合、岩石地球化学和地质年代学等系统研究表明,这些高压-超高压岩石均是早古生代( $\sim 500$  Ma)大陆深俯冲作用的产物(LIU et al., 2002, 2004, 2005, 2007; ZHANG et al., 2001, 2002, 2005a, 2011; 曹玉亭等, 2009, 2013; WANG et al., 2011)。最近,马拓等(2018)在南阿尔金西段新尤努斯萨依地区新发现了一套峰期变质时代为约 500 Ma 的高压变质的花岗质片麻岩,其峰期矿物组合为  $Grt + Ky + Pe (+ Ksp) + Ru + Qz$ , 变质温压条件为  $T > 950^{\circ}\text{C}$ ,  $P > 24$  kbar, 并结

合该片麻岩中包裹退变榴辉岩透镜体的地质观察,论证提出该高压花岗质片麻岩达到了榴辉岩相的变质条件。这一研究进一步拓展了南阿尔金高压-超高压岩石的时空分布,但目前关于这套花岗质片麻岩原岩的形成时代、属性与构造背景尚不清晰,其是否与南阿尔金淡水泉和英格利萨依两地高压或超高压花岗质片麻岩性质一致? 是否也是陆壳深俯冲作用的产物? 为此,笔者重点研究了该高压花岗质片麻岩原岩的形成时代与地球化学特征,以期进一步限定与讨论南阿尔金新发现的这套高压变质岩的构造地质意义。

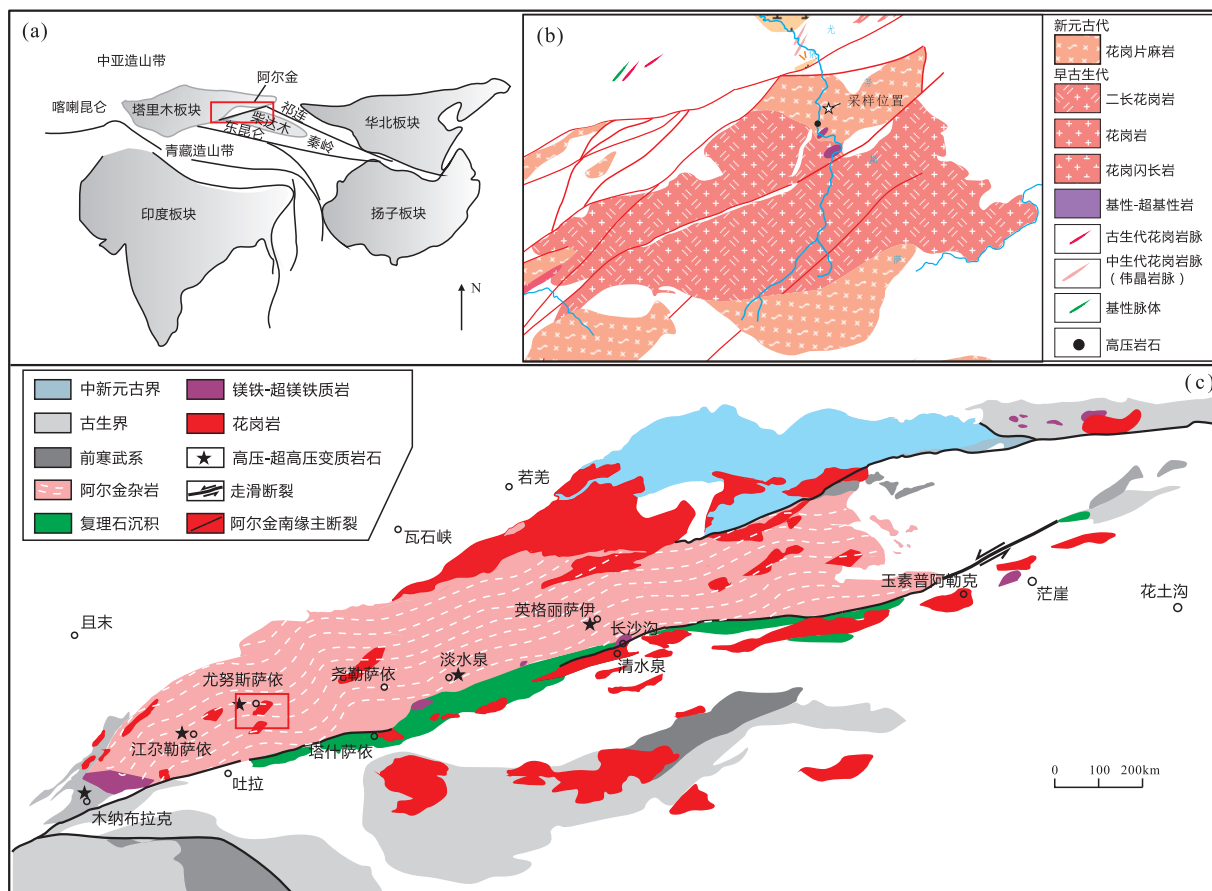


图 1 (a)阿尔金造山带构造位置简图(据 WANG et al., 2013 修编)(b)研究区地质图  
(c)阿尔金造山带地质简图(据 WANG et al., 2013 修编)

Fig. 1 (a) Location of Altyn Tagh and adjoining regions (Modified after WANG et al., 2013); (b) Geological map of the study areas; (c) Geological map of the Altyn Tagh (Modified after WANG et al., 2013)

## 1 区域构造背景和样品地质特征

阿尔金构造带经历了早古生代板块俯冲碰撞等

一系列复杂地质演化过程以及多期次相对应的岩浆活动,而后再被中、新生代多期次左行走滑断裂所截切,由不同时期、不同构造变动形成的不同构造环境的地质体共同组成的一个复合造山带(车自成等,

1995,1998;许志琴等,1999;刘良等,1999;崔军文等,1999;ZHANG et al.,1999,2001;LIU et al.,2009)。

前人综合区域地质特征、地层学、岩石学、地球化学及年代学的研究结果,将阿尔金造山带从北至南划分为阿北地块、红柳沟-拉配泉蛇绿混杂岩带、米兰河-金雁山地块和南阿尔金俯冲碰撞杂岩带等4个构造单元(图1c)(刘良,1999;许志琴等,1999;ZHANG et al.,2001;LIU et al.,2002)。

阿北地块主要由太古代麻粒岩相变质的中酸性-基性火山岩系、具孔兹岩系特征的变质岩系组成,包括斜长角闪岩、基性麻粒岩和长英质片麻岩等,其上不整合覆以中-新元古代蓟县系(新疆维吾尔自治区地质矿产局,1993)-青白口系(胡云绪等,2010)或南华系(LU et al.,2008);最近,王超等(2015)通过对比北阿尔金-敦煌地块、塔里木盆地西南缘铁克里克地块和阿拉善地块构造热事件,指出三者具有相似的古元古代地质演化历史。红柳沟-拉配泉构造混杂岩带发育有早古生代蛇绿岩,深海、半深海碎屑岩,碳酸盐岩、浅变质火山岩以及HP/LT变质岩等(车自成等,1995,2002;刘良,1999;杨经绥等,2002,2008;吴才来等,2005,2007;盖永升等,2015;刘锦宏,2017),其形成与洋壳俯冲碰撞及碰撞后伸展等构造环境有关。米兰河-金雁山地块地形上为阿尔金中央隆起带,其基底为中元古界大理岩和变砂岩,上覆蓟县系金雁山群厚层叠层石灰岩;新元古界索尔库里群与隆起带两侧不整合接触,由石英砂岩、鲕状和竹叶状灰岩、底砾岩组成,并富含叠层石灰岩(刘良等,1999)。

南阿尔金俯冲碰撞杂岩带可依据岩石组合及形成环境进一步划分为南阿尔金高压-超高压变质带(LIU et al.,2002,2004,2005,2007,2009,2012;张建新等,2002;ZHANG et al.,2005;曹玉亭等,2009)和阿帕-茫崖蛇绿混杂岩带(刘良等,1998;马中平等,2009,2011;李向民等,2009;杨文强等,2012)两部分。阿帕-茫崖蛇绿混杂岩带沿阿尔金南缘断裂带分布,主要由早古生代蛇绿岩残片、镁铁-超镁铁质岩与震旦一早寒武纪复理石沉积物组成(车自成等,2002;刘良等,1998,1999;王焰等,1999)。近年来,还陆续从中厘定出一套形成时代为~450 Ma,形成于碰撞后伸展背景下的非蛇绿岩端元的碰撞后镁铁-超镁铁质岩(马中平等,

2009,2011;董洪凯等,2014)。南阿尔金高压-超高压变质带内的高压-超高压变质岩石主要分布于江孜勒萨依、英格爾萨依、淡水泉及木纳布拉克等地区(刘良等,1999;LIU et al.,2002,2004,2005,2007,2009,2012;张建新等,1999,2002,2009;ZHANG et al.,2001,2005,2011;盖永升等,2017;曹玉亭等,2009,2013)。年代学研究表明,这些高压-超高压变质岩石的峰期变质时代为485~500 Ma(LIU et al.,2007,2009,2010,2012;WANG et al.,2011,2013;曹玉亭等,2009,2013;ZHANG et al.,2004,2005,2014)。

前人通过对南阿尔金不同区域花岗质片麻岩和高压基性岩石的研究,认为其原岩形成时代介于700~950 Ma,均为新元古代,提出原先划定为太古代或古一中元古代的阿尔金岩群应形成于新元古代(LIU et al.,2009,2012;WANG et al.,2011,2013),并且~900 Ma花岗质岩石的形成与罗迪尼亚超大陆事件引发的全球性岩浆活动相关。

笔者研究的花岗质片麻岩出露于南阿尔金高压-超高压变质岩带西段的尤努斯萨依地区。本次研究中的花岗质片麻岩即为花岗质高压麻粒岩,其变质级别达到榴辉岩相(马拓等,2018)。

## 2 野外地质与岩相学特征

尤努斯萨依地区主要发育有黑云斜长花岗岩、花岗质片麻岩、花岗闪长岩等、退变榴辉岩等;野外观察该花岗质片麻岩整体就位于南阿尔金杂岩中,岩石呈灰白色,表面球形风化明显;花岗质片麻岩为中细粒结构,受后期变质变形改造,片麻理明显,片麻理北北西向,产状 $55^{\circ}/70^{\circ}$ ,局部区域可见粗粒长石斑晶,岩体中可见多道细长石英脉体,可能为多期构造事件产物,岩体内部可见一系列顺片麻理方向分布的退变榴辉岩透镜体(图2)。岩相学观察显示,该花岗质片麻岩呈斑状变晶结构,主要变斑晶矿物有石榴子石、条纹长石等,局部区域可见石榴子石+蓝晶石+条纹长石+金红石等高压变质矿物组合;基质矿物主要为石英、钾长石或细粒条纹长石、斜长石和少量黑云母,偶见白云母。石榴子石含量约5%~10%,浑圆不等粒状;钾长石含量约30%,包括微斜长石和条纹长石2种,他形不等粒变斑晶状;斜长石含量约20%~25%;石英含量约35%,呈

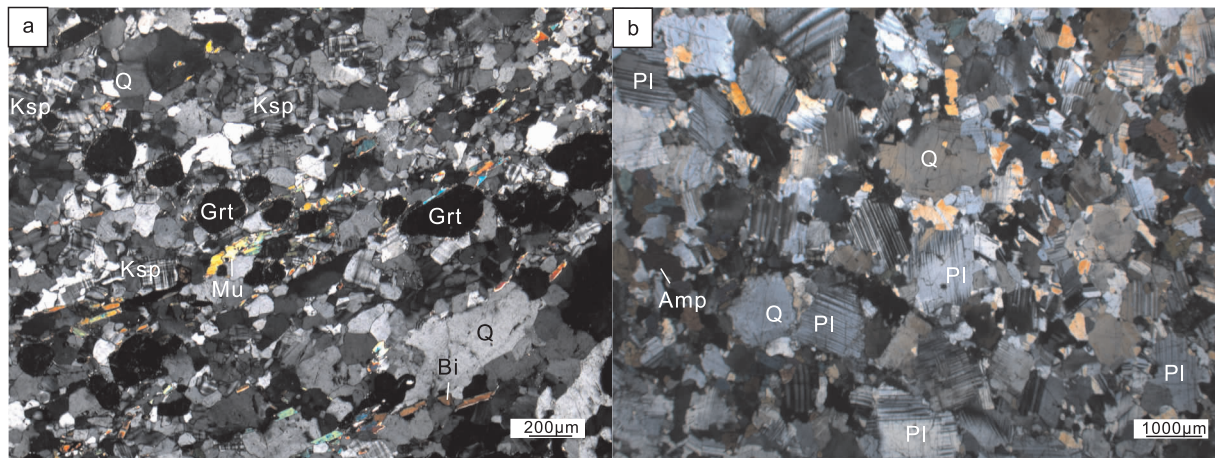
他形压扁不等粒状,部分颗粒顺片麻理被定向拉长;黑云母含量约5%,片状,沿片麻理方向排列;白云母含量较少,残余鳞片状;角闪石仅在个别小范围区域可见(图3)。马拓等(2018)通过细致的岩相学研究

与热力学模拟,指出该套花岗质片麻岩经历了峰期变质、高压麻粒岩相退变质、麻粒岩相-高角闪岩相退变质、角闪岩相退变质等4个阶段的变质演化过程,其峰期变质条件达到榴辉岩相。



图2 花岗质片麻岩野外露头照片

Fig. 2 Outcrop pictures of the granitic gneiss



Grt. 石榴子石;Ksp. 钾长石;Pl. 斜长石;Bi. 黑云母;Mu. 白云母;Q. 石英

图3 花岗质片麻岩镜下显微结构照片

Fig. 3 Microstructures of the granitic gneiss

### 3 样品分析方法

根据研究内容的需求,笔者采用了多种矿物学和地球化学分析的方法,包括全岩主微量元素分析、锆石 CL 图像分析以及锆石 LA-ICP-MS 微区定年和微量元素分析等,上述实验均在西北大学大陆动力学国家重点实验室完成。

全岩主量元素分析采用 X 射线荧光熔片法,测试在日本理学 RIX2100 X-射线荧光光谱仪上进行。而全岩主量元素分析采用溶液-等离子质谱法,利用美国 Elan 6100DRC 型电感耦合等离子质谱仪进行溶液测定。

挑选结晶度好、晶型完整的颗粒制成以环氧树脂为基础的样品靶并抛光至锆石最大横截面出露,应用装有英国 Gatan 公司生产的 MonoCL3<sup>+</sup> 阴极

荧光探测仪的电子显微扫描电镜完成锆石的 CL 图像的拍摄。锆石的 U-Pb 年龄测定和微量元素分析在 HewlettPackard 公司最新一代带装有 Shield-Torch 的 Agilent7500aICP-MS 和德国 Lambda-Physik 公司的 ComPex102ArF 激光器(波长 193 nm)以及 MicroLas 公司的 GeoLas200M 光学系统的联机上进行。激光束斑直径  $32\ \mu\text{m}$ , 激光剥蚀深度为  $20\ \mu\text{m}$ , 在一个点上同时完成微量元素和 U-Pb 同位素含量的测定。实验中采用氦气作为剥蚀物质的载气。采样方式为单点剥蚀, 数据采集选用一个质量峰一点的跳峰方式(peakjumping)。锆石年龄采用国际标准锆石 91500 作为外标标准物质, 元素含量采用 NIST610 作为外标,  $^{29}\text{Si}$  作为内标(锆石中  $\text{SiO}_2$  的含量为 32.8%)。每完成 5 个测点的样品测定加测 91500 标样一次, 每完成 10 个测点样品测定加测 NIST610、91500、GJ-1 标样各一次。样品的同位素比值及元素含量计算采用 ICPMSDataCal8.6 程序, 年龄计算及谐和图的绘制用 Isoplot2.49 完成。

详细分析步骤和数据处理方法参见文献 YUAN et al. (2004)。

## 4 地球化学特征

虽然先前研究表明尤努斯萨伊花岗质片麻岩普遍经历了高压变质作用, 但通过对变质过程的热力学模拟, 证明其变质过程在一个相对较干的体系进行, 峰期变质条件下熔流体比例  $\leq 5\%$  (马拓等, 2018), 表明其变质过程加入的熔流体成分极少; 同时, 在 Zr 与其他活动元素 (Na、Ca、K、Yb、Y、Nb 等) 二元图解(图 4)中, 这些活动元素均与 Zr 呈很好的线性关系, 亦表明其未受到变质过程中熔流体活动的影响。

因而, 笔者认为该花岗质片麻岩整体处于一个相对封闭的体系, 其地球化学属性应当与岩浆结晶时基本一致, 可以用来探讨花岗质原岩的地质属性。

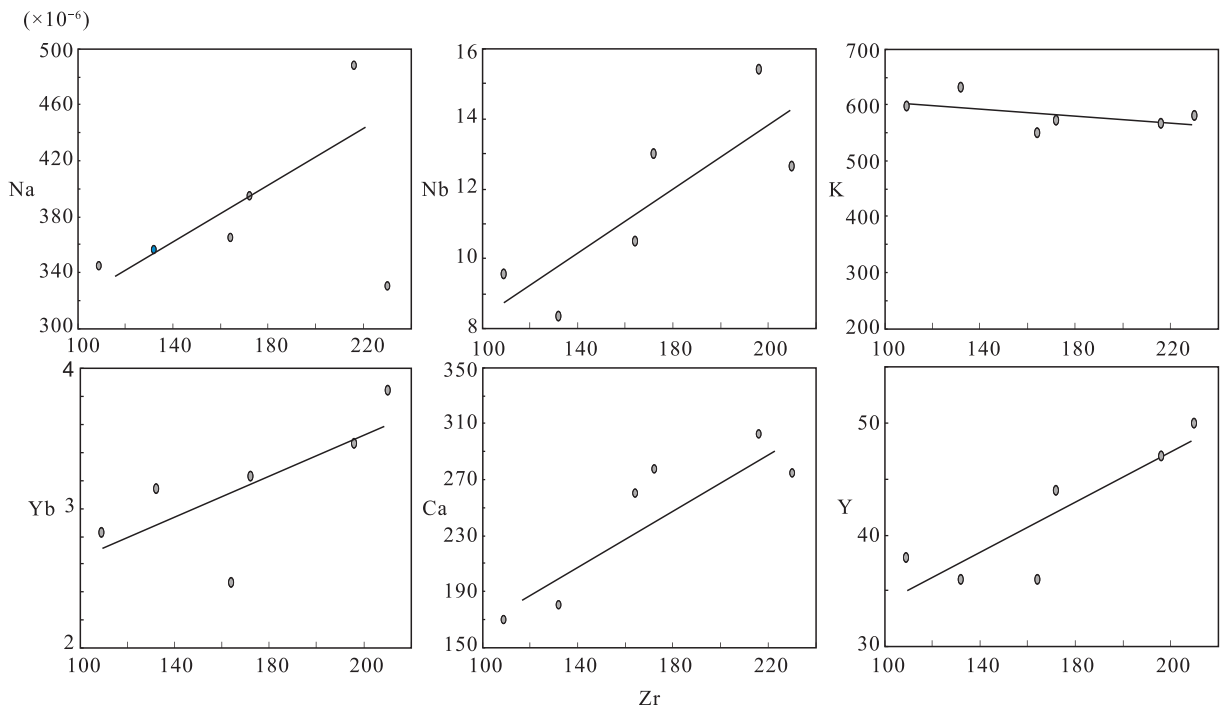


图 4 Zr 元素和其他活动元素二变量图解

Fig. 4 Diagram of two variables for Zr elements and other active elements

资料表明, 沉积岩和火成岩中  $\text{TiO}_2$  和  $\text{SiO}_2$  的含量均为负相关关系, 同  $\text{SiO}_2$  含量条件下, 沉积岩一般比火成岩含有更高的  $\text{TiO}_2$ , 在  $\text{TiO}_2$ - $\text{SiO}_2$  判别图

(J. Tarney, 1976)中, 样品落入火成岩范围(图 5a)。利用变异化学指数 ( $\text{CIA} = 100 * \text{Al}_2\text{O}_3 / (\text{Al}_2\text{O}_3 + \text{CaO} + \text{Na}_2\text{O} + \text{K}_2\text{O})$ ) 对花岗质片麻岩的原岩进行

判别,花岗质片麻岩的 CIA 为 59,同样指示它们的原岩为长英质的火成岩(NESBITT et al., 1982)。

尤努斯萨依花岗质片麻岩样品  $\text{SiO}_2 = 71.01\% \sim 75.07\%$ ,  $\text{Al}_2\text{O}_3 = 12.31\% \sim 14.21\%$ , 全碱  $\text{Na}_2\text{O} + \text{K}_2\text{O} = 7.44\% \sim 8.37\%$ ,  $\text{MgO} = 0.26\% \sim 0.60\%$ ,  $\text{FeO}^T = 1.75\% \sim 2.62\%$ ,  $\text{CaO} = 0.95\% \sim 1.70\%$ ,  $\text{TiO}_2 = 0.18\% \sim 0.34\%$ (表 1)。岩石样品铝饱和指数 A/CNK 值介于 1.03~1.16, A/NK =

1.25~1.50, 指示岩石主要为过铝质花岗岩(MANIAR et al., 1989)(图 5c)。岩石碱度率  $\text{AR} = 3.01 \sim 4.00$ , 里特曼指数  $\sigma = 1.74 \sim 2.50$ , 显示碱性-钙碱性系列岩石特征, 在  $\text{K}_2\text{O}-\text{SiO}_2$  图解(RICKWOOD, 1989)中岩石全部落入高钾钙碱性系列与钾玄岩系列过渡范围(图 5b), 在  $\text{SiO}_2-\text{AR}$  图解(WRIGHT, 1969)中样品全部落入碱性岩石范围内(图 5d)。

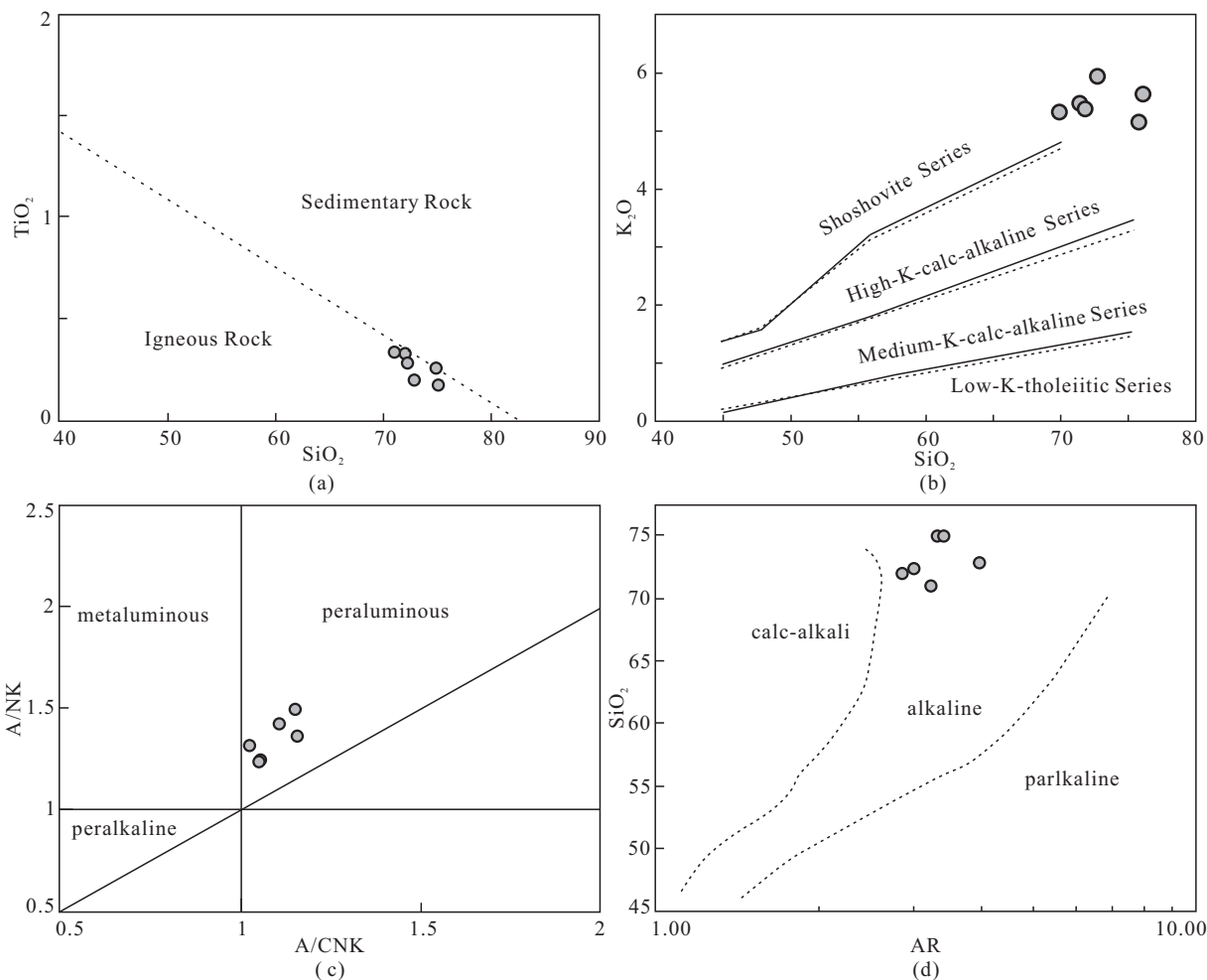


图 5 花岗质片麻岩主量元素分析图解 (a)  $\text{TiO}_2$ - $\text{SiO}_2$  图解(J. Tarney, 1976); (b)  $\text{K}_2\text{O}-\text{SiO}_2$  判别图解(RICKWOOD, 1989); (c) A/NK-A/CNK 图解(MANIAR et al., 1989); (d)  $\text{SiO}_2$ -AR 判别图解(WRIGHT, 1969)

Fig. 5 Major element diagrams of granitic gneiss (a)  $\text{TiO}_2$ - $\text{SiO}_2$  diagram (J. Tarney, 1976); (b)  $\text{K}_2\text{O}-\text{SiO}_2$  diagram (RICKWOOD, 1989); (c) A/NK-A/CNK diagram (MANIAR et al., 1989); (d)  $\text{SiO}_2$ -AR diagram (WRIGHT, 1969)

稀土元素分析结果显示岩石样品的  $\sum_{\text{REE}}$  总量为  $131.15 \times 10^{-6} \sim 234.34 \times 10^{-6}$ , 平均值为  $184.13 \times 10^{-6}$ ;  $\sum_{\text{LREE}}$  总量为  $110.49 \times 10^{-6} \sim 206.69 \times 10^{-6}$ ;  $\sum_{\text{HREE}}$  总量为  $19.97 \times 10^{-6} \sim 28.48 \times 10^{-6}$ 。岩石各样品具有一致的右倾“V”型稀土配分模式

(图 6a), 均表现出明显的 LREE 富集 ( $\text{LREE}/\text{HREE} = 5.07 \sim 7.67$ ,  $(\text{La}/\text{Yb})_{\text{N}} = 4.82 \sim 9.58$ ) 和强烈 Eu 亏损 ( $\delta_{\text{Eu}} = 0.42 \sim 0.63$ ) 特征, 显示出典型的地壳重熔型花岗岩的稀土组成特征。

微量元素原始地幔标准化蛛网图(图 6a)显示

表 1 花岗质片麻岩主量元素(wt%)及微量元素( $\times 10^{-6}$ )化学组成表Tab. 1 Major elements (wt%) and trace elements ( $\times 10^{-6}$ ) compositions of the granitic gneiss

Spe. No	A95-1	A95-2	A95-3	A95-4	A95-5	A95-6	Spe. No	A95-1	A95-2	A95-3	A95-4	A95-5	A95-6
SiO <sub>2</sub>	74.89	71.01	72.24	71.98	72.86	75.07	Ho	1.040	1.430	1.310	1.540	1.100	1.210
TiO <sub>2</sub>	0.260	0.340	0.290	0.330	0.200	0.180	Er	2.760	3.760	3.460	4.140	3.100	3.140
Al <sub>2</sub> O <sub>3</sub>	12.31	14.21	14.1	13.97	12.6	13.17	Tm	0.390	0.540	0.500	0.600	0.470	0.450
Fe <sub>2</sub> O <sub>3</sub> <sup>T</sup>	2.410	2.910	2.630	2.910	2.000	1.950	Yb	2.470	3.460	3.230	3.840	3.140	2.830
MnO	0.010	0.040	0.040	0.040	0.030	0.030	Lu	0.320	0.450	0.410	0.510	0.400	0.350
MgO	0.400	0.540	0.450	0.600	0.300	0.260	Hf	3.920	5.250	4.340	5.740	3.710	3.150
CaO	1.460	1.700	1.560	1.540	1.010	0.950	Ta	0.750	0.990	1.010	0.550	0.830	0.780
Na <sub>2</sub> O	2.260	3.030	2.450	2.050	2.210	2.140	Pb	22.50	23.10	24.80	18.78	42.00	20.50
K <sub>2</sub> O	5.180	5.340	5.400	5.490	5.960	5.650	Th	11.84	14.41	13.69	15.33	4.840	3.400
P <sub>2</sub> O <sub>5</sub>	0.120	0.150	0.140	0.150	0.120	0.130	U	1.500	1.810	2.360	1.990	4.280	2.030
LOI	0.440	0.300	0.400	0.440	2.390	0.570	Na <sub>2</sub> O+K <sub>2</sub> O	7.440	8.370	7.850	7.540	8.170	7.790
Total	99.74	99.57	99.70	99.50	99.68	100.1	FeO <sup>T</sup>	2.169	2.618	2.366	2.618	1.800	1.755
Li	23.10	37.00	15.13	31.00	23.30	19.79	A/CNK	1.028	1.026	1.109	1.153	1.057	1.159
Be	1.060	1.060	0.840	0.580	2.770	0.670	A/NK	1.320	1.320	1.428	1.500	1.249	1.367
Sc	5.350	7.170	6.570	7.210	5.020	4.150	FeO <sup>T</sup> /MgO	5.421	4.849	5.259	4.364	5.999	6.749
V	19.34	28.40	22.70	25.40	14.96	11.66	Al <sub>2</sub> O <sub>3</sub> /TiO <sub>2</sub>	47.35	41.79	48.62	42.33	63.00	73.17
Cr	22.60	17.56	17.87	26.00	12.67	13.80	CaO/Na <sub>2</sub> O	0.646	0.561	0.637	0.751	0.457	0.444
Co	60.00	59.00	69.00	72.00	72.00	69.00	K <sub>2</sub> O/Na <sub>2</sub> O	2.292	1.762	2.204	2.678	2.697	2.640
Ni	7.160	7.410	7.180	12.380	5.830	6.230	AR	3.351	3.220	3.010	2.892	4.004	3.461
Cu	0.020	<0.000	2.600	<0.000	<0.000	1.820	$\sigma$	1.736	2.501	2.107	1.962	2.235	1.892
Zn	29.70	64.00	62.00	50.00	46.00	61.00	$\sum_{\text{REE}}$	166.1	224.7	205.5	208.9	122.9	124.3
Ga	17.53	21.60	21.00	20.80	17.42	17.72	$\sum_{\text{LREE}}$	153.1	206.7	189.1	191.0	110.7	110.5
Rb	235.0	225.0	244.0	243.0	305.0	332.0	$\sum_{\text{HREE}}$	12.99	18.01	16.45	17.85	12.25	13.80
Sr	92.00	103.00	98.00	112.0	72.00	68.00	LREE/HREE	11.79	11.48	11.49	10.70	9.036	8.007
Y	36.00	47.00	44.00	50.00	36.00	38.00	(La/Yb) <sub>N</sub>	10.16	9.329	8.883	7.659	5.117	5.931
Zr	164.0	216.0	172.0	230.0	132.0	109.0	$\delta_{\text{Eu}}$	0.625	0.609	0.630	0.582	0.416	0.511
Nb	10.50	15.41	13.03	12.67	8.350	9.570	Th/U	7.893	7.961	5.801	7.704	1.131	1.675
Cs	0.820	0.780	1.210	0.770	8.010	2.470	Zr/Hf	41.84	41.14	39.63	40.07	35.58	34.60
Ba	804.0	849.0	835.0	835.0	474.0	499.0	Nb/Ta	14.00	15.57	12.90	23.04	10.06	12.27
La	35.00	45.00	40.00	41.00	22.40	23.40	K/Rb	183.0	197.0	183.7	187.6	162.2	141.3
Ce	74.00	99.00	91.00	92.00	54.00	52.00	La/Nb	3.333	2.920	3.070	3.236	2.683	2.445
Pr	8.260	11.490	10.530	10.600	6.140	6.240	Sr/Ba	0.114	0.121	0.117	0.134	0.152	0.136
Nd	28.70	41.00	38.00	38.00	22.30	22.60	Mg <sup>#</sup>	27.89	30.19	28.51	32.46	25.90	23.71
Sm	5.930	8.520	7.930	7.930	5.140	5.330	La/Yb	14.17	13.01	12.38	10.68	7.134	8.269
Eu	1.220	1.680	1.600	1.510	0.710	0.920	Fe-number	0.822	0.805	0.817	0.788	0.836	0.852
Gd	6.010	8.350	7.600	7.930	5.280	5.690	MALI	5.980	6.670	6.290	6.000	7.160	6.840
Tb	0.970	1.340	1.240	1.330	0.920	1.070	ASI	1.028	1.026	1.109	1.153	1.057	1.159
Dy	6.010	8.320	7.610	8.590	6.050	7.040							

注: Mg<sup>#</sup> = Mg<sup>2+</sup> / (Mg<sup>2+</sup> + Fe<sup>2+</sup>) × 100;  $\sigma$  = (Na<sub>2</sub>O + K<sub>2</sub>O) \* 2 / (SiO<sub>2</sub> - 43); AR = [Al<sub>2</sub>O<sub>3</sub> + CaO + (Na<sub>2</sub>O + K<sub>2</sub>O)] / [Al<sub>2</sub>O<sub>3</sub> + CaO(Na<sub>2</sub>O + K<sub>2</sub>O)]; R<sub>1</sub> = 4Si - 11(Na + K) - 2(Fe + Ti); R<sub>2</sub> = 6Ca + 2Mg + Al; A/MF = Al<sub>2</sub>O<sub>3</sub> / (FeO<sup>T</sup> + MgO) (mol); C/MF = CaO / (FeO<sup>T</sup> + MgO) (mol); A/CNK = Al<sup>2</sup>O<sub>3</sub> / (CaO + K<sub>2</sub>O + Na<sub>2</sub>O)。



出明显的 Nb-Ta 亏损,相对富集 Rb、Th、La 等大离子亲石元素而亏损 Ba、Ta、Nb、Sr、Ti 等(图 6b),元素的丰度特征与典型陆-陆碰撞 S 型花岗岩(PEARCE et al., 1984)相似。样品 Th/U=1.13

~7.96(平均值为 5.36), Zr/Hf=34.60~41.84(平均值为 38.81),稍高于上地壳平均值(Th/U=4.2, Zr/Hf=~37, GAO et al., 1998),显示出上地壳沉积物重熔的特征。

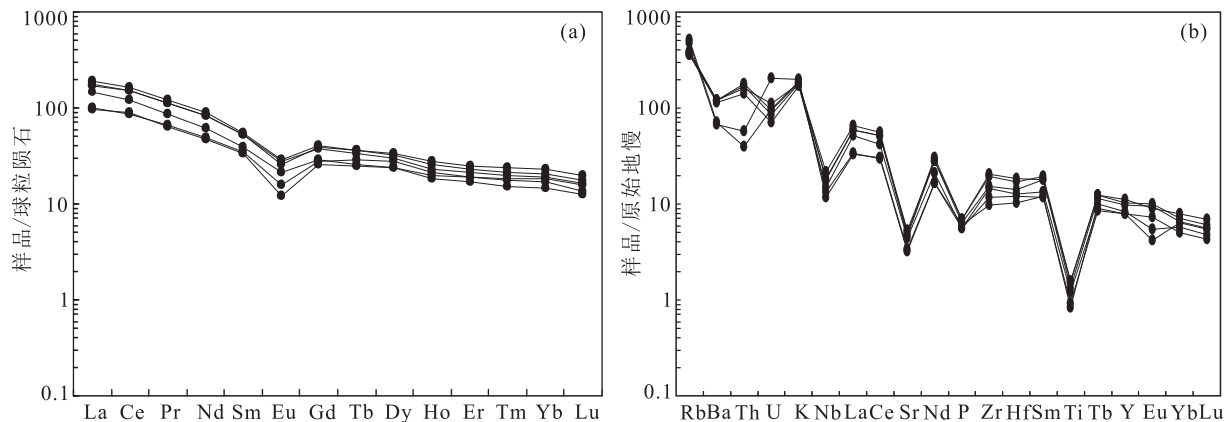


图 6 (a) 全岩球粒陨石标准化稀土配分图(标准化值据 TAYLOR et al., 1985);(b) 全岩微量元素原始地幔标准化蛛网图(标准化值据 SUN et al., 1989)

Fig. 6 (a) Chondrite-normalized REE patterns (Normalization values after TAYLOR et al., 1985) for granitic gneiss; (b) Primitive-mantle normalized spider diagram (Normalization values after SUN et al., 1989) for granitic gneiss

## 5 锆石 U-Pb 年代学

马拓等(2018)曾对尤努斯萨依地区这套花岗质片麻岩具有典型高压变质矿物组合的样品进行了年代学研究,初步获得了(900.2±4.1) Ma 的原岩年龄和(497.8±2.7) Ma 的峰期变质年龄。笔者则挑选尤努斯萨依地区花岗质片麻岩中变质程度相对较低的样品中的锆石进行了重新测试。

本次研究的花岗质片麻岩中锆石颗粒较大,直径约 100~200 μm。阴极发光(CL)显示锆石具有明显的六边形形态,部分锆石呈板条状。所有锆石都发育有良好的成分环带,显示明显的岩浆锆石特点,未见明显变质成因的边部(图 7a)。

对尤努斯萨依花岗质片麻岩进行了 15 个原位微区的锆石微量元素测试,所得结果见图 7c 和表 2。锆石核部稀土元素总量为  $803 \times 10^{-6} \sim 2\,541 \times 10^{-6}$ ,重稀土总量为  $815 \times 10^{-6} \sim 1\,911 \times 10^{-6}$ , $(Gd/Yb)_N$  值在 0.02~0.08,在球粒陨石标准化稀土配分图显示重稀土富集的配分特征;Th/U 值落于 0.1~0.9,符合岩浆锆石特征。

年龄谐和图(图 7b)显示,尤努斯萨伊花岗质片

麻岩 15 个核部测点年龄(表 3)均落在谐和线附近,构成一个年龄集中区,其加权平均值为(899.7±4.0) Ma;结合锆石 CL 图像与锆石微量元素特征,笔者认为上述年龄均代表其花岗质岩浆的结晶年龄。

## 6 讨论

### 6.1 原岩的物源分析

实验岩石学数据表明,在一定的温度压力条件下,过铝质花岗质熔体可以来源于多种源岩的部分熔融(RAPP et al., 1991; RAPP et al., 1995; JOHANNES et al., 1996; WINTHER et al., 1991),其成分变化取决于初始熔融物质的成分、含水量差异以及温压条件。因此,判别强过铝质花岗岩的源岩性质成为判别构造环境的关键。目前,南阿尔金地区已报到的新元古代花岗质岩石普遍为上地壳杂砂岩熔融产物(王超等, 2006; 王立社等, 2015),而李琦等(2015)通过研究则发现南阿尔金南缘帕夏拉依档盖里克(886.5±5) Ma 的花岗质岩体为下地壳角闪岩部分熔融形成的产物。

表 2 LA-ICP-MS trace element compositions of zircons ( $10^{-6}$ )

样品号	La	Ce	Pr	Nd	Sm	Eu	Gd	Tb	Dy	Ho	Er	Tm	Yb	Lu
A95-01	0.018	1.060	0.054	1.206	4.023	0.110	27.42	9.613	121.5	41.49	186.2	35.13	357.0	58.95
A95-02	0.017	1.015	0.051	0.995	3.183	0.177	28.23	12.30	170.0	63.06	288.1	56.96	598.6	96.83
A95-03	1.204	8.561	0.990	8.641	10.005	1.403	54.83	18.56	237.4	87.60	410.7	78.77	840.4	140.3
A95-04	0.094	3.617	0.095	1.959	3.230	0.378	26.92	11.94	184.4	79.38	418.1	85.68	946.2	158.9
A95-05	0.064	5.959	0.351	6.269	11.065	1.406	58.70	18.94	230.8	83.59	378.9	71.62	737.8	119.4
A95-06	0.366	2.008	0.168	1.014	1.645	0.100	15.27	8.337	127.6	50.09	246.1	49.93	533.0	90.24
A95-07	0.129	0.741	0.016	0.407	1.615	0.006	16.87	8.844	130.4	51.54	253.8	51.25	555.2	92.97
A95-08	0.026	0.531	0.028	0.674	1.307	0.065	15.65	8.369	112.6	41.49	197.1	37.95	402.1	65.51
A95-09	0.279	1.434	0.083	0.507	1.500	0.110	22.95	11.14	155.2	56.62	253.7	48.19	499.6	80.96
A95-10	0.127	1.236	0.084	1.643	4.794	0.159	30.58	10.67	121.1	41.52	182.6	32.98	332.1	53.36
A95-11	0.028	1.100	0.103	1.957	5.247	0.195	33.96	11.53	138.3	47.44	206.3	37.80	382.1	62.20
A95-12	0.332	3.598	0.156	2.170	5.087	0.342	34.20	14.89	211.4	84.78	425.0	83.89	900.5	151.1
A95-13	0.488	2.507	0.143	1.870	3.889	0.277	32.14	10.89	128.6	42.15	178.3	32.19	326.4	52.44
A95-14	0.559	6.345	0.235	3.380	6.026	0.407	46.59	19.63	279.9	114.7	581.1	115.5	1257	206.9
A95-15	0.000	1.319	0.026	1.077	4.145	0.454	35.66	11.67	158.0	54.73	231.4	43.03	447.3	70.25

表 3 LA-ICP-MS 锆石 U-Pb 同位素年代学分析结果表

Tab. 3 LA-ICP-MS U-Pb zircons age data

样品号	含量 ( $10^{-6}$ )		同位素比值												
	$^{232}\text{Th}$	$^{238}\text{U}$	Th/U	$^{207}\text{Pb}/^{206}\text{Pb}$	$1\sigma$	$^{207}\text{Pb}/^{235}\text{U}$	$1\sigma$	$^{206}\text{Pb}/^{238}\text{U}$	$1\sigma$	$^{207}\text{Pb}/^{206}\text{Pb}$	$1\sigma$	$^{207}\text{Pb}/^{235}\text{U}$	$1\sigma$	$^{206}\text{Pb}/^{238}\text{U}$	$1\sigma$
A95-01	57.95	175.1	0.33	0.0684	0.0020	1.4208	0.0536	0.1496	0.0012	883	61	898	22	898	7
A95-02	46.85	296.1	0.16	0.0665	0.0023	1.3746	0.0458	0.1495	0.0016	820	73	878	20	898	9
A95-03	149.2	227.9	0.65	0.0707	0.0022	1.5044	0.0459	0.1526	0.0016	950	62	932	19	916	9
A95-04	65.90	174.8	0.38	0.0655	0.0026	1.3535	0.0521	0.1490	0.0018	791	83	869	22	895	10
A95-05	207.9	240.9	0.86	0.0674	0.0019	1.4102	0.0458	0.1501	0.0013	850	57	893	19	901	7
A95-06	33.83	409.7	0.08	0.0676	0.0015	1.4194	0.0480	0.1502	0.0010	857	44	897	20	902	6
A95-07	31.50	409.4	0.08	0.0683	0.0015	1.4255	0.0600	0.1496	0.0016	877	45	900	25	899	9
A95-08	40.63	614.2	0.07	0.0633	0.0015	1.3116	0.0636	0.1484	0.0016	720	18	851	28	892	9
A95-09	58.27	723.2	0.08	0.0679	0.0012	1.4147	0.0554	0.1493	0.0010	865	37	895	23	897	5
A95-10	63.67	172.1	0.37	0.0684	0.0022	1.4087	0.0496	0.1493	0.0018	881	67	893	21	897	10
A95-11	70.67	172.8	0.41	0.0681	0.0021	1.4066	0.0450	0.1488	0.0016	872	66	892	19	894	9
A95-12	91.92	332.6	0.28	0.0699	0.0019	1.4553	0.0425	0.1495	0.0013	928	53	912	18	898	7
A95-13	63.42	179.5	0.35	0.0721	0.0023	1.5086	0.0519	0.1508	0.0018	987	63	934	21	906	10
A95-14	135.6	376.8	0.36	0.0692	0.0013	1.4475	0.0451	0.1500	0.0012	903	38	909	19	901	7
A95-15	71.97	226.4	0.32	0.0617	0.0039	1.2779	0.0798	0.1498	0.0027	665	137	836	36	900	15

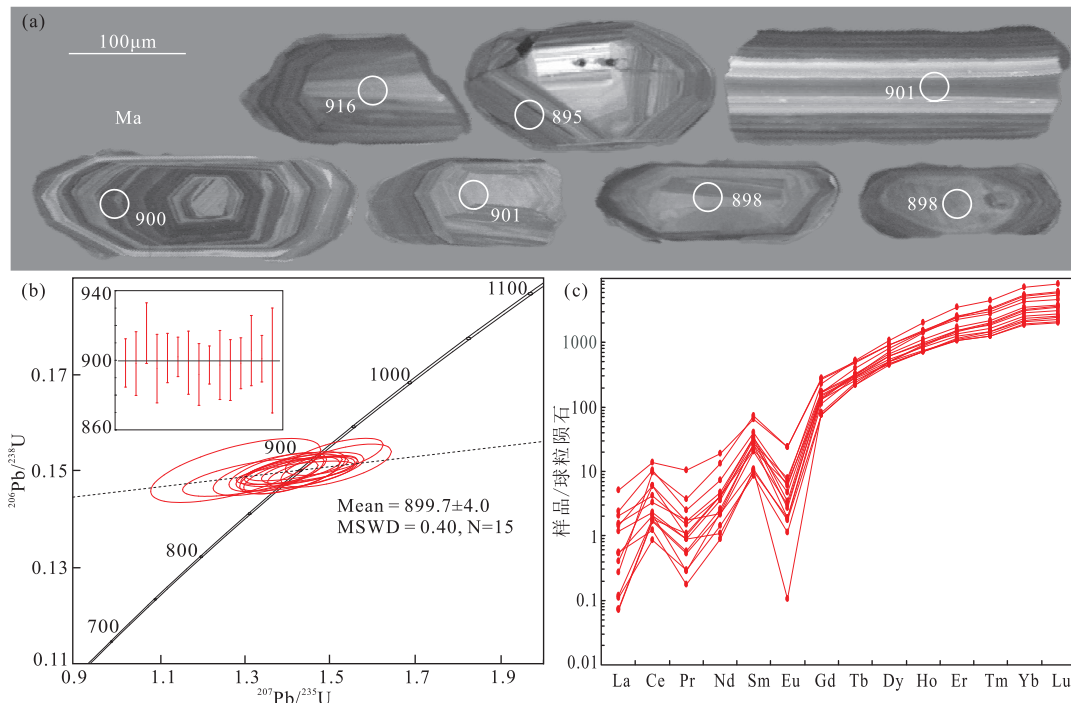


图7 (a) 锆石阴极发光图像;(b) 锆石 U-Pb 年龄谱和图;(c) 稀土元素球粒陨石标准化配分图  
(标准化据 SUN et al. ,1989)

Fig. 7 (a) CL images; (b) U-Pb ages Concordia diagram; (c) Chondrite-normalized REE pattern for zircons (Normalization after SUN et al. ,1989)

笔者研究的花岗质片麻岩样品稀土总量平均值为  $184.13 \times 10^{-6}$ , Nb 含量为  $8.35 \times 10^{-6} \sim 15.41 \times 10^{-6}$ , Ta 含量为  $0.55 \times 10^{-6} \sim 1.01 \times 10^{-6}$ ,  $(La/Yb)_N = 5.12 \sim 10.16$  (平均值为 7.85),  $Nb/Ta = 10.06 \sim 15.57$ ,  $K/Rb = 141 \sim 197$ ,  $La/Nb = 2.45 \sim 3.33$  (平均值为 2.95),  $\delta_{Eu}$  (0.42 ~ 0.63) 平均为 0.56, 稀土元素球粒陨石标准化呈右倾的“V”型模式, 与上述地壳岩石中的相应值基本一致 ( $Nb = 8 \times 10^{-6} \sim 11.5 \pm 2.6 \times 10^{-6}$ ,  $Ta = 0.7 \times 10^{-6} \sim (0.92 \pm 0.12) \times 10^{-6}$ ,  $Nb/Ta = 12 \sim 13$ ,  $K/Rb = 150 \sim 3501$ ,  $La/Nb = 2.2$  (BARTH et al. , 2000; DOSTAL et al. , 2000), 也与前人研究的阿尔金普遍发育的壳源型花岗岩基本特征一致 (王超等, 2006; 王立社等, 2015; 陈红杰, 2018)。样品在  $Nb/Ta-Nb$  和  $La/Nb-Nb$  图解 (BARTH et al. , 2000) (图 8) 中均落于上地壳平均值周围, 具有典型的上地壳属性。

$Mg^\#$  值的高低是判断岩浆熔体来源的重要指标, 可用来指示岩石源区是否经历了壳幔混合作用,  $Mg^\# < 40$  时认为是地壳部分熔融形成的熔体, 而  $Mg^\#$  较高的则可能有幔源物质的加入 (RAPP et al. , 1995)。本次研究样品具有较低的  $Mg^\#$  值

(23.7 ~ 32.5, 平均值为 28.1), 表明该套花岗岩主要来源于地壳物质的部分熔融。

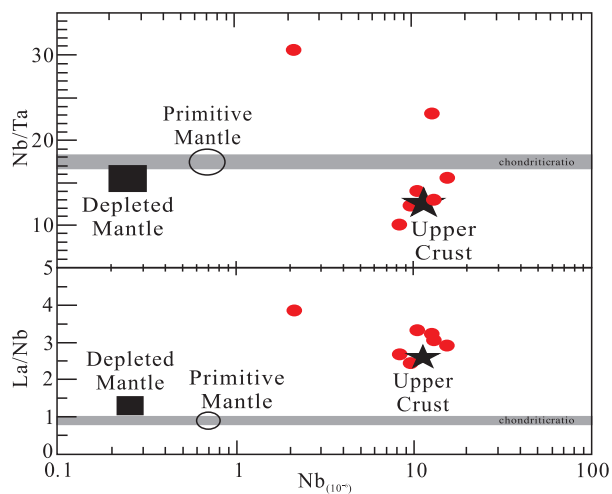


图8  $Nb/Ta-Nb$  和  $La/Nb-Nb$  图解 (Upper Crust 据 BARTH et al. , 2000; Chondritic ratios gray bars 据 JOCHUM et al. , 1997 和 MCDONOUGH et al. , 1995; Depleted mantle 据 JOCHUM et al. , 1998)

Fig. 8  $Nb/Ta-Nb$  and  $La/Nb-Nb$  diagram for granitic gneiss (BARTH et al. , 2000; JOCHUM et al. , 1997, 1998; MCDONOUGH et al. , 1995)

利用  $\text{CaO}/(\text{MgO} + \text{FeO}^{\text{T}}) - \text{Al}_2\text{O}_3/(\text{MgO} + \text{FeO}^{\text{T}})$  图解 (ALThER et al., 2000) (图 9a) 进行判别, 样品均落于杂砂岩部分熔融区域; 在  $\text{Al}_2\text{O}_3 + \text{FeO}^{\text{T}} + \text{MgO} + \text{TiO}_2 - \text{Al}_2\text{O}_3/(\text{FeO}^{\text{T}} + \text{MgO} + \text{TiO}_2)$  图解 (DOUCE, 2000) 中, 样品均落入砂质岩区域 (图 9b); 在  $\text{Rb}/\text{Sr}-\text{Rb}/\text{Ba}$  图解 (SYLVESTER, 1998) 中, 样品均落入砂屑岩源区 (图 9d)。前人研究显示, 由泥质类源岩水饱和熔融产生的铝长英质岩浆高  $\text{Sr}/\text{Ba}$  (0.5~1.6) 与正 Eu 异常, 来自于富粘土而贫斜长石的泥质岩源岩熔体的具

有较低的  $\text{CaO}/\text{Na}_2\text{O}$  (<0.3), 而来自于富斜长石而贫粘土的砂屑质源岩熔体的  $\text{CaO}/\text{Na}_2\text{O}$  值较高 (>0.3) (HARRIS et al., 1992; SYLVESTER, 1998)。本次研究样品的  $\text{Sr}/\text{Ba}$  值 (0.11~0.15) 很低, 具有负 Eu 异常,  $\text{CaO}/\text{Na}_2\text{O} = 0.44 \sim 0.75 > 0.3$  (图 9c), 显示源岩并非泥质类岩石而可能为陆壳沉积的砂质岩。

综上所述, 可以认为笔者研究的尤努斯萨依花岗质片麻岩的源岩为上地壳杂砂岩沉积物。

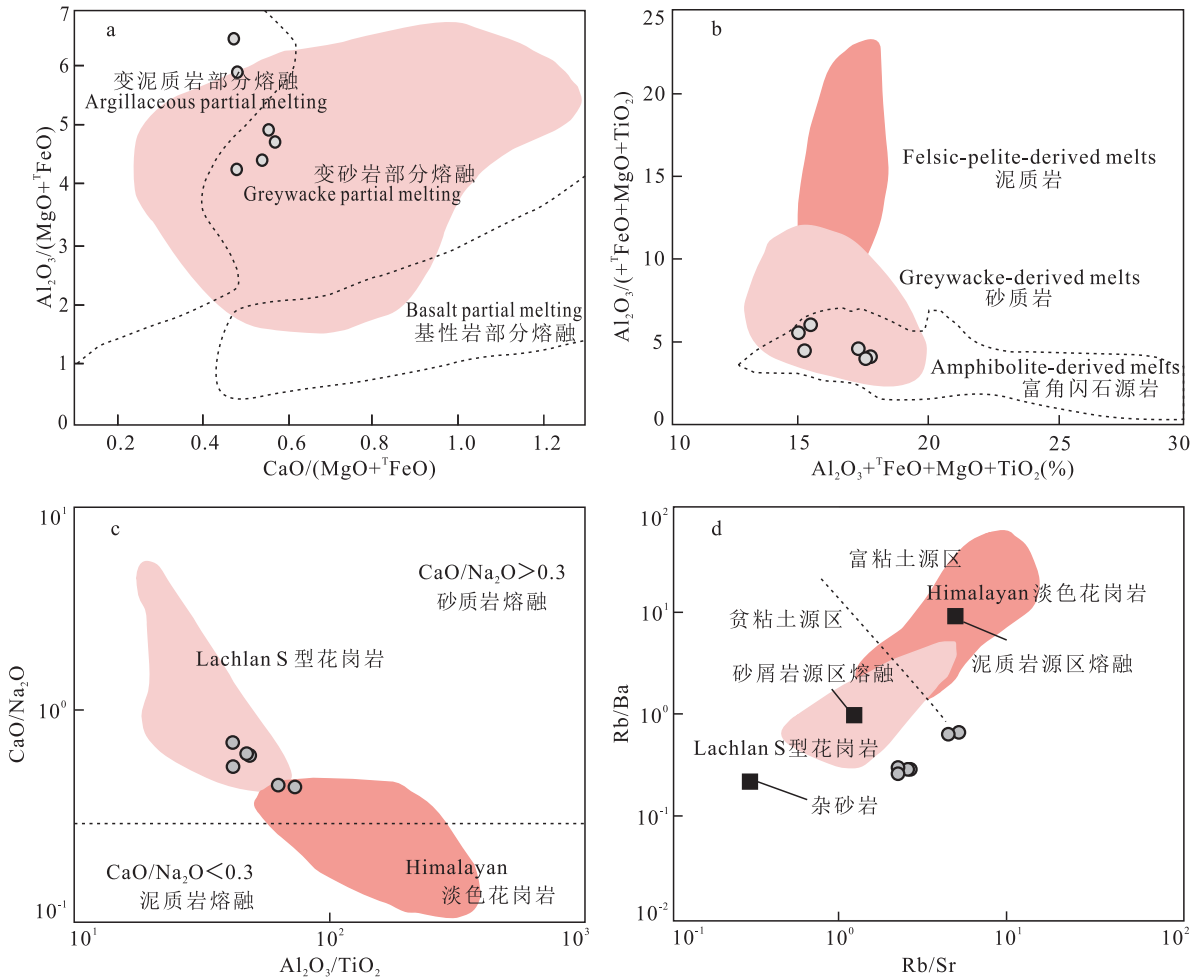


图 9 (a)  $\text{Al}_2\text{O}_3/(\text{MgO} + \text{FeO}^{\text{T}}) - \text{CaO}/(\text{MgO} + \text{FeO}^{\text{T}})$  成因图解 (据 ALThER et al., 2000); (b)  $\text{Al}_2\text{O}_3 + \text{FeO}^{\text{T}} + \text{MgO} + \text{TiO}_2 - \text{Al}_2\text{O}_3/(\text{FeO}^{\text{T}} + \text{MgO} + \text{TiO}_2)$  图解 (据 DOUCE, 2000); (c)  $\text{Al}_2\text{O}_3/\text{TiO}_2 - \text{CaO}/\text{Na}_2\text{O}$  图解; (d)  $\text{Rb}/\text{Sr}-\text{Rb}/\text{Ba}$  图解 (据 SYLVESTER, 1998). Himalayan 淡色花岗岩数据来源于 SEARLE et al. (1986), INGER et al. (1993), AYRES et al. (1997); Lachlan S 型花岗岩数据来源于 Chappell and Simpson (1984), HEALY et al. (2004)。

Fig. 9 (a)  $\text{Al}_2\text{O}_3/(\text{MgO} + \text{FeO}^{\text{T}}) - \text{CaO}/(\text{MgO} + \text{FeO}^{\text{T}})$  diagram (After ALThER et al., 2000); (b)  $\text{Al}_2\text{O}_3 + \text{FeO}^{\text{T}} + \text{MgO} + \text{TiO}_2 - \text{Al}_2\text{O}_3/(\text{FeO}^{\text{T}} + \text{MgO} + \text{TiO}_2)$  diagram (After DOUCE, 2000); (c)  $\text{Al}_2\text{O}_3/\text{TiO}_2 - \text{CaO}/\text{Na}_2\text{O}$  diagram; (d)  $\text{Rb}/\text{Sr}-\text{Rb}/\text{Ba}$  diagram (After SYLVESTER, 1998)

## 6.2 原岩岩浆形成的温度压力条件

由于大部分花岗岩浆是绝热式上升就位的,那么岩浆在早期结晶时的温度可近似代表岩浆起源时温度的最小值(吴福元, 2007)。而锆石是花岗质岩浆体系中较早结晶且在地质事件中具有较高的化学和物理稳定性及抗干扰能力的副矿物,锆石中 Zr 和 Ti 2 个元素的分配系数主要受到温度的控制,实验岩石学数据表明锆石结晶温度与 Zr 或 Ti 的含量具有特定的函数关系,因而可以通过相应的温度计来计算锆石结晶温度(CALVIN et al., 2003),目前,2 种比较成熟的方法是锆石饱和温度计算及锆石钛温度计。

依据锆石饱和温度计(WATSON et al., 1983)及锆石钛温度计(WATSON et al., 2006)进行计算,本次研究分别获得了 785~861℃ 和 735~881℃ 的结果(表 4),二者基本一致,故而认为该岩石原岩结晶温度为 785~861℃。

此外,还有研究表明,在升温熔融过程中,含 Ti 矿物相对更容易分解,使融体中 Ti 含量增多,故而  $Al_2O_3/TiO_2$  值的大小可以在一定程度上反映部分熔融温度的高低。SYLVERSTER(1998)通过 Ti 含量的高低对熔融温度做出了大致区分,当  $Al_2O_3/TiO_2$  大于 100 时,其熔融温度小于 875℃;  $Al_2O_3/TiO_2$  小于 100,其熔融温度大于 875℃。尤努斯萨伊花岗质片麻岩的相应比值为 41~74,表明其熔融温度可能达到 875℃ 以上,高于其平均结晶温度。

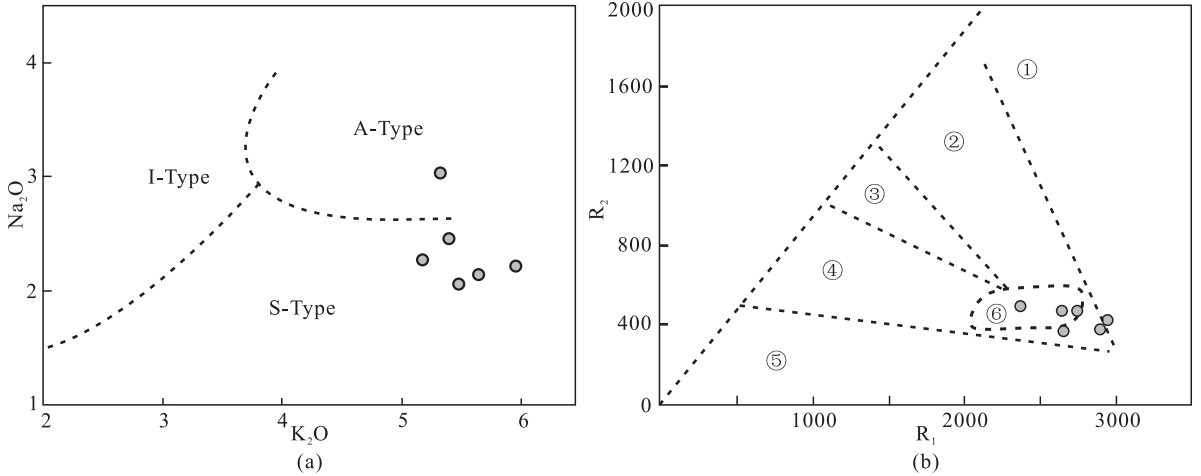
对压力条件估算一般依据源区残留相矿物。实验岩石学资料表明,石榴子石残留代表岩浆源区的压力较高(>10 kbar),而斜长石的残留则指示岩浆起源的压力较低(DEFANT et al., 1990)。同时, Sr、Yb 等微量元素及其比值对花岗岩压力的研究具有重要的指示意义。高 Sr (>  $300 \times 10^{-6}$ ) 和无负 Eu 异常表明源区残留相中基本无斜长石,低 Y (<  $15 \times 10^{-6}$ )、高 Sr/Y (>20)、低 Yb (<  $1.9 \times 10^{-6}$ ) 和高 La/Yb (>20) 指示源区残留相中有石榴子石(张旗, 2006, 2010; CASTILLO et al., 2006)。该岩石具有低 Sr ( $68.0 \times 10^{-6} \sim 112.0 \times 10^{-6}$ )、负 Eu 异常、高 Y ( $36.0 \times 10^{-6} \sim 50.0 \times 10^{-6}$ )、低 Sr/Y (1.79~2.56)、较高 Yb ( $2.47 \times 10^{-6} \sim 3.84 \times 10^{-6}$ ) 以及低 La/Yb (7.13~14.17) 等特征,均说明了源区残留相中有斜长石无石榴子石,因此该岩石原岩岩浆源区的压力较低。

## 6.3 原岩形成的构造环境

花岗岩作为特定地质背景下的产物,它的岩石学、矿物学和地球化学特点能够反映它形成时的构造环境。尤努斯萨依花岗质片麻岩原岩高硅、富碱、低钙、低镁、过铝质的碱性花岗岩的特征与区内及邻区报道的 S 型花岗岩元素特征相同。依据 FORST 等(2001)利用铁指数( $Fe\text{-number} = FeO/(FeO + MgO)$ )、钙碱指数( $MALI = K_2O + Na_2O - CaO$ )和铝饱和指数( $ASI = Al/(Ca - 1.67P + Na + K)$ )等参数对花岗岩进行地球化学分类的方案,尤努斯萨依花岗质片麻岩的  $Fe\text{-number} = 0.79 \sim 0.85$ ,  $MALI = 5.98 \sim 7.16$ ,  $ASI = 1.42 \sim 1.58 (> 1.1)$ , 与方案中定义的壳源同构造碰撞型花岗岩的特征一致。结合 BARBARIN(1999)的花岗岩类分类,属于镁质、钙碱性、壳源过铝质花岗岩,亦表明其为大陆碰撞环境的产物。岩石的  $FeO^T/MgO = 4.36 \sim 6.75$ ,  $Al_2O_3/TiO_2 = 41.79 \sim 73.17$ ,  $CaO/Na_2O = 0.44 \sim 0.75$ ,  $K_2O/Na_2O = 1.76 \sim 2.70$ , 与地壳沉积岩部分熔融形成的 S 型花岗岩地球化学特征 ( $SiO_2 < 74\%$ 、 $Al_2O_3/TiO_2 < 100$ 、 $CaO/Na_2O > 0.3$ 、 $K_2O/Na_2O > 1$ ) 一致(路凤香等, 2002)。

$R_1 - R_2$  构造环境判别图解(图 10b)对花岗岩构造环境可以进行较好的区分,该图解显示原岩花岗岩成因与同碰撞或造山作用有关。在  $Na_2O - K_2O$  图解(图 10a)中,样品投影也落入 S 型花岗岩区,表明其应该为碰撞造山的产物。在 Nb-Y 和 Rb-Yb+Ta 等花岗岩构造环境识别图解(图 11)中,该样品也落入板内花岗岩或同构造的碰撞花岗岩区域内。

众所周知,罗迪尼亚超大陆是距今 10 亿年左右全球范围内 Grenville 造山运动形成的超大陆,其最终汇聚时限约在 900 Ma,并在约 800 Ma 之后迅速解体。前人研究已在阿尔金及其周缘地区(库鲁克塔格、柯坪、铁克里克、柴北缘、北山、中祁连、昆中断裂带等地)报道了大量形成时代为 0.8~1.1 Ga 的新元古代早期与汇聚碰撞事件有关的花岗岩类(LU et al., 1999; 梅华林等, 1999; 郭进京等, 1999; 陆松年, 2002; GEHRELS et al., 2003; 王超等, 2006; SONG et al., 2012; WANG et al., 2013)。结合这一区域背景与尤努斯萨依花岗质片麻岩的年代学研究,作者认为尤努斯萨依花岗质片麻岩的地球化学特征显示其具有地壳熔融型、同碰撞花岗岩的特点,是新元古代的 Rodinia 超大陆汇聚阶段不同块体碰撞的产物。



①. 地幔分异产物; ②. 板块碰撞前花岗岩; ③. 碰撞后隆起花岗岩; ④. 造山晚期花岗岩; ⑤. 非造山花岗岩;  
⑥. 同碰撞花岗岩; ⑦. 造山后花岗岩

图 10 (a)Na<sub>2</sub>O - K<sub>2</sub>O 图解 (ROLLISON, 1993); (b)R<sub>1</sub> - R<sub>2</sub> 构造环境判别图解 (BATCHELOR et al. , 1985)

Fig. 10 Granitics gneiss, stectonic settings discrimination diagram (BATCHELOR et al. , 1985)

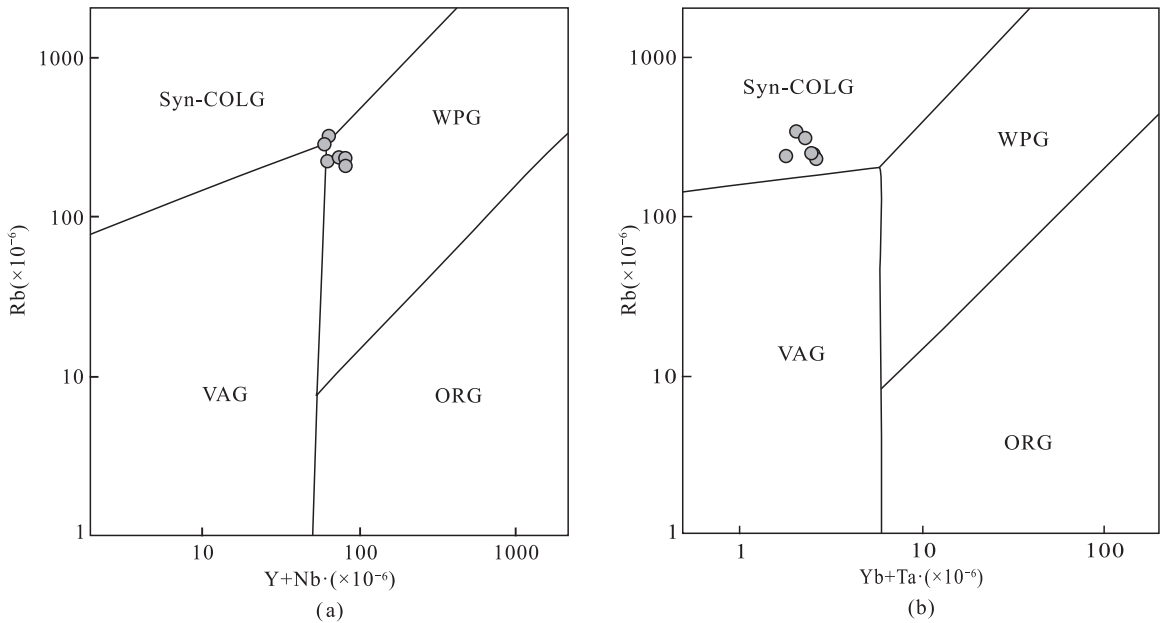


图 11 (a)花岗岩 Nb-Y 图解和 (b)Rb-Yb+Ta 图解 (据皮尔斯, 1984)

Fig. 11 (a) Nb-Y diagram and (b) Rb-(Yb+Ta) diagram for granitics gneiss (PEARCE et al. , 1984)

### 6.4 构造地质意义

(1) 先前研究认为阿尔金岩群是塔里木板块太古代—古元古代结晶基底的一部分 (RGXR, 1993; 崔军文等, 1999; HE et al. , 2012; LONG et al. , 2011, 2012; MA et al. , 2012a, b), 但 WANG et al (2013) 通过对南阿尔金江孜勒萨依、淡水泉、巴什瓦克、亚干布阳等地花岗质质岩石年代学的研究, 指出以花岗质片麻岩为主体的阿尔金岩群其形成时代应

该为新元古代。尤努斯萨依 ~900 Ma 花岗质片麻岩的发现为这一结论提供了新的区域年代学数据。

(2) 尤努斯萨依高压花岗质片麻岩原岩的形成时代为约 900 Ma, 该年龄值远大于其发生高压变质的时代 (~500 Ma), 表明其原岩就位于地壳约 400 Ma 之后才发生俯冲遭受高压变质作用, 时间间隔远大于一个威尔逊旋回 (</= 200 Ma) 的时限。因此, 说明其原岩的形成与其发生高压变质作用应分

属于 2 个性质完全不同的构造地质事件的产物。结合前述分析,前者可能对应于新元古代 Rodinia 超大陆的汇聚地质事件,后者则是南阿尔金早古生代陆壳俯冲-深俯冲作用的产物。

表 4 锆石饱和温度计及锆石 Ti 温度计计算结果表

Tab. 4 Values for sample by zircon saturation thermometer and Ti for zircon thermometer

样品号	锆石饱和温度计			
	Zr( $\times 10^{-6}$ )	M(比值)	$D_{Zr}$	$T_{Zr}$ ( $^{\circ}\text{C}$ )
A95-2	216	1.45	229.6	820
A95-3	172	1.31	288.4	803
A95-4	230	1.26	215.7	824
A95-5	132	1.34	375.8	784
A95-6	109	1.21	455.0	861

样品号	锆石 Ti 温度计		
	Ti( $\times 10^{-6}$ )	年龄(Ma)	$T_{Ti}$ ( $^{\circ}\text{C}$ )
A95-01	9.991	898	805
A95-02	6.629	898	766
A95-03	10.72	916	812
A95-04	7.558	895	778
A95-05	11.31	901	818
A95-06	6.256	902	760
A95-07	4.878	899	738
A95-08	4.695	892	735
A95-09	13.51	897	836
A95-10	10.03	897	805
A95-11	12.28	894	826
A95-12	9.031	898	795
A95-13	13.20	906	833
A95-14	9.494	901	800
A95-15	20.42	900	881

注:  $T_{Zr}$ ( $^{\circ}\text{C}$ ) =  $12\ 900 / [\ln D_{Zr} + 0.85M + 2.95] - 273.15$  (Watson and Harrison, 1983);  $D_{Zr}$  =  $496\ 000 / \text{全岩锆含量}$ ,  $M$  =  $(2\text{Ca} + \text{K} + \text{Na}) / (\text{Si} \times \text{Al})$ ;  $T_{Ti}$ ( $^{\circ}\text{C}$ ) =  $5\ 080 / [5.711 - \lg(\text{Ti})] - 273.15$  (FERRY et al., 2007)。

(3)前人已研究报道南阿尔金淡水泉地区高压变质的花岗质片麻岩原岩的形成时代为(866 $\pm$ 5) Ma,原岩具有 S 型花岗岩的地球化学特征(朱小辉等, 2014);英格利萨伊超高压的花岗质片麻岩(LIU et al., 2004; ZHANG et al., 2004)的形成时代为 810~885 Ma,原岩亦具有 S 型花岗岩的地球化学特征。显然,尤努斯萨依高压花岗质片麻岩的原岩与南阿尔金淡水泉地区高压变质的花岗质片麻岩以及英格利萨伊超高压的花岗质片麻岩(具有

几乎一致的原岩形成时代和地球化学特征,表明它们具有相同的原岩属性。但值得特别关注的是,中阿尔金及其南缘江孜勒萨依剖面北部、亚干布阳、中阿尔金环形山、帕夏拉依档盖里克等地还发育有未记录变质事件的新元古代花岗质岩石(王超等, 2006; WANG et al., 2013; 王立社等, 2015; 陈红杰, 2018; 李琦等, 2018),说明这些没有明显深变质记录的新元古代花岗质岩石可能并没有参与到南阿尔金早古生代的大陆俯冲-深俯冲作用之中,可能位于俯冲带的上盘。

## 7 结论

(1)南阿尔金尤努斯萨依花岗质片麻岩为镁质、钙碱性、过铝质岩石,其的地球化学特征显示其具有地壳熔融型、同碰撞 S 型花岗岩的特点。

(2)南阿尔金尤努斯萨依高压变质花岗质片麻岩的原岩形成于新元古代,年龄为(899.7 $\pm$ 4.0) Ma,其所代表的构造岩浆事件可能与阿尔金及其周缘广泛报道的新元古代 Rodinia 超大陆的汇聚时间相关。同时,进一步限定以花岗质片麻岩为主体的阿尔金杂岩的形成时代应为早新元古代。

(3)南阿尔金尤努斯萨依高压花岗质片麻岩原岩的形成时代为约 900 Ma,该年龄值远大于其发生高压变质的时代(~500 Ma),表明其原岩就位于地壳约 400 Ma 之后才发生俯冲遭受高压变质作用,时间间隔远大于一个威尔逊旋回( $\leq$ 200 Ma)的时限,显然,该高压岩石的形成是陆壳俯冲作用的产物,为进一步限定南阿尔金早古生代陆壳俯冲-深俯冲作用提供了新的依据。

## 参考文献(References):

- 盖永升,刘良,康磊,等.北阿尔金蛇绿混杂岩带中斜长花岗岩的成因及其地质意义[J].岩石学报,2015,31(9):2549-2565.
- GAI Yongsheng, LIU Liang, KANG Lei, et al. The origin and geologic significance of plagiogranite in ophiolite belt at North Altyn Tagh[J]. Acta Petrologica Sinica, 2015, 31(9):2549-2565.
- 盖永升,刘良,王超,等.南阿尔金榴辉岩中首次发现柯石英[J].矿物岩石地球化学通报,2017,62(15):

- 1048-1051.
- GAI Yongsheng, LIU Liang, WANG Chao, et al. Discovery of coesite in eclogite from Keqike Jianggalesayi: New evidence for ultrahigh-pressure metamorphism in South Altyn Tagh, northwestern China[J]. *Science Bulletin*, 2017, 62(15): 1048-1051
- 郭进京, 赵凤清, 李怀坤. 中祁连东段晋宁期碰撞型花岗岩及其地质意义[J]. *地球学报*, 1999, 20(1): 10-15.
- GUO Jinjing, ZHAO Fengqing, LI Huaikun. Jinningian Collisional Granite Belt in the Eastern Sector of the Central Qilian Massif and Its Implication[J]. *Acta Geoscientia Sinica*, 1999, 20(1) : 10-15.
- 董洪凯, 郭金城, 陈海燕, 等. 新疆阿尔金地区长沙沟一带奥陶纪侵入岩及其演化特征[J]. *西北地质*, 2014, 47(04): 73-87.
- DONG Hongkai, GUO Jincheng, CHEN Haiyan, et al. Evolution Characteristics of Ordovician Intrusive Rock in Changshagou of Altun Region[J]. *Northwestern Geology*, 2014, 47(04):73-87.
- 路凤香, 桑隆康. 岩石学[M]. 北京:地质出版社, 2002, 82-94.
- LU Fengxiang, SANG Longkang. *Petrology*[M]. Beijing: Geological Publishing House, 2002: 82-94.
- 刘锦宏. 阿尔金拉配泉地区火成岩的组合、地球化学、年代学及其构造意义[D]. 西安:西北大学 2017.
- LIU Jinhong. The associations, geochronology and geochemistry of igneous rocks in Lapeiquan, North Altyn Tagh and Its tectonic significance[D]. Xi'an: Northwest University, 2017.
- 刘良, 车自成. 阿尔金茫崖地区早古生代蛇绿岩的 Sm - Nd 等时线年龄证据[J]. *科学通报*, 1998, 8:880-883.
- LIU Liang, CHE Zicheng. evidence of Sm-Nd isochron age for the early Paleozoic ophiolite in Mangya area, Altun Mountains [J]. *Chinese Science Bulletin*, 1998, 43: 754-756.
- 刘良, 车自成, 王焰, 等. 阿尔金高压变质岩带的特征及其构造意义[J]. *岩石学报*, 1999, 15(1):57-64.
- LIU Liang, CHE Zicheng, WANG Yan, et al. The petrological characters and geotectonic setting of high-pressure metamorphic rock belts in Altun Mountains [J]. *Acta Petrologica Sinica*, 1999, 15(1): 57-64 (in Chinese with English abstract).
- 李琦, 曾忠诚, 陈宁, 等. 阿尔金造山带青白口纪亚干布阳片麻岩年龄、地球化学特征及其地质意义[J]. *地质通报*, 2018, 37(4):642-654
- LI Qi, ZENG Zhongcheng, CHEN Ning, et al. Zircon U-Pb ages, geochemical characteristics and geological significance of Yaganbuyang gneiss in Qingbaikou period along the Altun orogenic belt [J]. *Acta Petrologica Sinica*, 2018, 37(4):642-654
- 李向民, 马中平, 孙吉明, 等. 阿尔金断裂南缘约马克其镁铁-超镁铁岩的性质和年代学研究[J]. *岩石学报*, 2009, 25(4):862-872.
- LI Xiangmin, MA Zhongping, SUN Jiming, et al. Characteristics and age study about the Yuemakeqi mafic-ultramafic rock in the southern Altyn Fault [J]. *Acta Petrologica Sinica*, 2009, 25(4):862-872.
- 马中平, 李向民, 孙吉明, 等. 阿尔金山南缘长沙沟镁铁-超镁铁质层状杂岩体的发现与地质意义—岩石学和地球化学初步研究[J]. *岩石学报*, 2009, 25(4):793-804.
- MA Zhongping, LI Xiangmin, SUN Jiming, et al. Discovery of layered mafic-ultramafic intrusion in Changshagou, Altyn Tagh, and its geological implication: A pilot study on its petrological and geochemical characteristics [J]. *Acta Petrologica Sinica*, 2009, 25(4):793-804.
- 马中平, 李向民, 徐学义, 等. 南阿尔金山清水泉镁铁超镁铁质侵入体 LA-ICP-MS 锆石 U-Pb 同位素定年及其意义 [J]. *中国地质*, 2011, 38(4):1071-1078.
- MA Zhongping, LI Xiangmin, XU Xueyi, et al. Zircon LA-ICP-MS U-Pb isotopic dating for Qingshuiquan layered maficulmafic intrusion southern Altun orogen, in northwestern China and its implication [J]. *Geology in China*, 2011, 38(4):1071-1078.
- 马拓, 刘良, 盖永升, 等. 南阿尔金尤努斯萨依花岗质高压麻粒岩的发现及其地质意义 [J]. *岩石学报*, 2018, 34(12):3643-3657
- MA Tuo, LIU Liang, GAI Yongsheng, et al. Discovery of the high pressure granitic granulite in South Altyn and it's geological significance [J]. *Acta Petrologica Sinica*, 2018, 34(12):3643-3657.
- 梅华林, 李惠民, 陆松年, 等. 甘肃柳园地区花岗质岩石时代及成因 [J]. *岩石矿物学杂志*, 1999, 18(1):14-17.
- MEI Hualin, LI Huimin, LU Songnian, et al. The Age and Origin of the Liuyuan Granitoid, Northwestern Gansu [J]. *Acta Petrologica et Mineralogica*, 1999, 18(1): 14-17.



- 新疆维吾尔自治区地质矿产局. 中华人民共和国地质矿产部地质专报[M]. 北京:地质出版社, 1993.
- 杨经绥, 吴才来, 史仁灯. 阿尔金山米兰红柳沟的席状岩墙群:海底扩张的重要证据[J]. 地质通报, 2002, (2): 69-74.
- YANG Jingsui, WU Cailai, SHI Rendeng. Sheeted dike swarm in Hongliugou, northwest of the Altyn region: Evidence for seafloor spreading[J]. Geological Bulletin Of China, 2002, (2):69-74.
- 杨经绥, 史仁灯, 吴才来, 等. 北阿尔金地区米兰红柳沟蛇绿岩的岩石学特征和 SHRIMP 定年[J]. 岩石学报, 2008, 24(7):1567-1584.
- YANG Jingsui, SHI Rendeng, WU Cailai, et al. Petrology and SHRIMP age of the Hongliugou ophiolite at Milan, north Altyn, at the northern margin of the Tibetan plateau[J]. Acta Petrologica Sinica, 2008, 24(7):1567-1584.
- 杨文强, 刘良, 丁海波, 等. 南阿尔金迪木那里克花岗岩地球化学、锆石 U-Pb 年代学与 Hf 同位素特征及其构造地质意义[J]. 岩石学报, 2012, 28(12):4139-4150.
- YANG Wenchang, LIU Liang, DING Haibo, et al. Geochemistry, geochronology and zircon Hf isotopes of the Dimunalike granite in South Altyn Tagn and its geological significance[J]. Acta Petrologica Sinica, 2012, 28(12):4139-4150.
- 杨文强, 丁海波, 刘良, 等. 新疆阿尔金南部迪木那里克铁矿赋矿地层的形成时代及其地质意义[J]. 地质通报, 2012, 31(12):2090-2101.
- YANG Wenchang, DING Haibo, LIU Liang, et al. Formation age of ore-bearing strata of the Dimunalike iron deposit in South Altun Mountains and its geological significance[J]. Geological Bulletin of China, 2012, 31(12): 2090-2101.
- 吴才来, 杨经绥, 姚尚志, 等. 北阿尔金巴什考供盆地南缘花岗杂岩体特征及锆石 SHRIMP 定年[J]. 岩石学报, 2005, (3):846-858.
- WU Cailai, YANG Jingsui, YAO Shangzai, et al. Characteristics of the granitoid complex and its zircon SHRIMP dating at the south margin of the Bashikaogong Basin, North Altyn, NW China[J]. Acta Petrologica Sinica, 2005, (3): 846-858.
- 吴才来, 姚尚志, 曾令森, 等. 北阿尔金巴什考供-斯米尔布拉克花岗杂岩特征及锆石 SHRIMP-U-Pb 定年[J]. 中国科学(D辑:地球科学), 2007, (1):10-26.
- 王立社, 张巍, 段星星, 等. 阿尔金环形山花岗片麻岩同位素年龄及成因研究[J]. 岩石学报, 2015, 31(1)-0119-32.
- WANG Lishe, ZHANG Wei, DUAN Xingxing, et al. Isotopic age and genesis of the monzogranitic gneiss at the Huanxingshan in middle Altyn Tagh[J]. Acta Petrologica Sinica, 2015, 31(1)-0119-32.
- 王焰, 刘良, 车自成, 等. 阿尔金茫崖地区早古生代蛇绿岩的地球化学特征[J]. 地质论评, 1999, 45(增刊1): 1010-1014.
- WANG Yan, LIU Liang, CHE Zicheng, et al. Geochemical Characteristics Of Early Paleozoic Ophiolite In Mangnai Area, Altyn Mountains[J]. Geologocal Review, 1999, 45(Suppl. 1):1010-1014.
- 王超, 刘良, 杨文强, 等. 北阿尔金-敦煌地块太古代-古元古代地壳生长和改造:来自锆石 U-Pb 年代学的研究[J]. 地质论评, 2015, 61(增刊):718-719.
- 王超, 刘良, 车自成, 等. 阿尔金南缘榴辉岩带中花岗片麻岩的时代及构造环境探讨[J]. 高校地质学报, 2006, 12(1):74-82.
- WANG Chao, LIU Liang, CHE Zicheng, et al. U-Pb Geochronology and Tectonic Setting of the Granitic Gneiss in Jianggaleisayi Eclogite Belt, the Southern Edge of Altyn Tagh[J]. Geological Journal of China Universities, 2006, 12(1):74-82.
- 曹玉亭, 刘良, 王超, 等. 阿尔金淡水泉早古生代泥质高压麻粒岩及其 P-T 演化轨迹[J]. 岩石学报, 2009, 25(9): 2260-2270.
- CAO Yuting, LIU Liang, WANG Chao, et al. P-T path of Early Paleozoic pelitic high-pressure granulite from Danshuiquan area in Altyn Tagh[J]. Acta Petrologica Sinica, 2009, 25(9):2260-2270.
- 曹玉亭, 刘良, 王超, 等. 南阿尔金木纳布拉克地区高压泥质麻粒岩的确定及其地质意义[J]. 岩石学报, 2013, 29(5):1727-1739.
- CAO Yuting, LIU Liang, WANG Chao, et al. Determination and implication of the HP pelitic granulite from the Munabulake area in the South Altyn Tagh[J]. Acta Petrologica Sinica, 2013, 29(5):1727-1739.
- 朱小辉, 曹玉亭, 刘良, 等. 阿尔金淡水泉花岗质高压麻粒岩 P-T 演化及年代学研究[J]. 岩石学报, 2014, 30(12): 3717-3728.
- ZHU Xiaohui, CAO Yuting, LIU Liang, et al. P-T path and geochronology of high pressure granitic granulite

- from Danshuiquan area in Altyn Tagh[J]. *Acta Petrologica Sinica*, 2014, 30(12): 3717-3728.
- 陈丹玲, 刘良. 北秦岭榴辉岩及相关岩石年代学的进一步确定及其对板片俯冲属性的约束 [J]. *地学前缘*, 2011, 18(2): 158-169.
- CHENG Danlin, LIU Liang. New data on the chronology of eclogite and associated rock from Guanpo Area, North Qinling orogeny and its constraint on nature of North Qinling HP-UHP eclogite terrane [J]. *Earth Science Frontiers*, 2011, 18(2): 158-169.
- 车自成, 刘良, 刘洪福, 等. 阿尔金山地区高压变质泥质岩石的发现及其产出环境 [J]. *科学通报*, 1995, (14): 1298-1300.
- CHE Zicheng, LIU Liang, LIU Hongfu, et al. Discovery and occurrence of high- pressure metapelitic rocks from Altun Mountain area, Xinjiang Autonomous Region [J]. *Chinese Science Bulletin*, 1995, 40(23): 1988-1991.
- 车自成, 刘良, 刘洪福, 等. 阿尔金断裂系的组成及相关中生代含油气盆地的成因特征 [J]. *中国区域地质*, 1998, 17(4): 377-384.
- CHE Zicheng, LIU Liang, LIU Hongfu, et al. The constitutions of the Altyn fault system and genetic characteristics of related Meso-Cenozoic petroleum-bearing basin [J]. *Regional Geology of China*, 1998, 17(4): 377-384 (in Chinese with English abstract).
- 车自成, 刘良, 罗金海. 中国及其邻区区域大地构造学 [M]. 北京: 科学出版社, 2002.
- CHE Zicheng, LIU Liang, LUO Jinhai. *Geotectonics of China and Its Adjacent Regions* [M]. Beijing: Science Press (in Chinese), 2002.
- 崔军文, 李莉, 李朋武. 青藏高原北缘的深部构造 [A]. 1999年中国地球物理学会年刊-中国地球物理学会第十五届年会论文集 [C], 1999, 542.
- 许志琴, 杨经绥, 张建新, 等. 阿尔金断裂两侧构造单元的对比及岩石圈剪切机制 [J]. *地质学报*, 1999, 73(3): 193-205.
- XU Zhiqin, YANG Jingsui, ZHANG Jianxin, et al. A Comparison Between The Tectonic Units On The Two Sides Of The Altun Sinistral Strike-Slip Fault And The Mechanism Of Lithospheric Shearing [J]. *Acta Geologica Sinica*, 1999, 73(3): 193-205.
- 胡云绪, 校培喜, 高晓峰, 等. 东昆仑西段—阿尔金地区区域地层划分及地层时空格架建立 [J]. *西北地质*, 2010, 43(04): 152-158.
- HU Yunxu, XIAO Peixi, GAO Xiaofeng, et al. Division and Space-Time Frame Foundation of Regional Stratum in the Western Sector of East Kunlun and the Altun Region [J]. *Northwestern Geology*, 2010, 43 (04): 152-158.
- ALTHER R, HOLL A, HEGNER E, et al. High potassium, calc-alkaline I-type plutonism in the European Variscides: Northern Vosges (France) and northern Schwarzwald (Germany) [J]. *Lithos*, 2000, 50(1-3): 51-73.
- AYRES M, HARRIS N. REE fractionation and Nd-isotope disequilibrium during crustal anatexis: constraints from Himalayan leucogranites [J]. *Chem. Geol*, 1997, 139(1-4): 249-269
- BARBARIN B. A review of there lation ships between granitoid types, their origins and their geodynamic environments [J]. *Lithos*, 1999, 46: 605-626.
- BARTH M G, MCDONOUGH W F, RNDNICK RI. Tracking the budget of Nb and Ta in the continental crust [J]. *Chem. Geol*, 2000, 165(3-4): 197-213.
- BATCHELOR RA, BOWDEN P. Petrogenetic interpretation of granitoid rock series using multicationic parameters [J]. *Chem. Geol*, 1985, 48(1-4): 43-55.
- CALVIN FM, MCDowell SM, Mapes RW. Hot and cold granites implications of zircon saturation temperatures and preservation of Inheritance [J]. *Geology*, 2003, 31(6): 529-532.
- CASTILLO PR. An overview of adakite petrogenesis [J]. *Chinese Science Bulletin*, 2006, 51(3): 257-268
- GUO Zhaojie, ZHANG Zhicheng, WANG Jianjun. Sm-Nd isochron age of ophiolite along northern margin of Altun Tagh Mountain and its tectonic significance [J]. *Chinese Science Bulletin*, 1999, 44(15): 456-458.
- CHAPPELL BW, SIMPSON PR. Source Rocks of I- and S-Type Granites in the Lachlan Fold Belt, Southeastern Australia; Discussion [J]. *Philosophical Transactions of The Royal Society B Biological Sciences*, 1984, 310(1514): 706-707.
- CHEN Danling, LIU Liang, SUN Yong, et al. Felsic veins within UHP eclogite at xitieshan in North Qaidam, NW China; Partial melting during exhumation [J]. *Lithos*, 2012, 136-139: 187-200.

- CHOPIN C. Coesite and pure pyrope in high-grade blueschists of the Western Alps: a first record and some consequences [J]. *Contributions to Mineralogy and Petrology*, 1984, 86(2): 107-118.
- CUI Junwen, LI Li, LI Pengwu. Deep structure of the northern edge of the Tibetan plateau[A]. *Annual journal of the Chinese geophysical society (in Chinese) [C]*, 1999.
- DEFANT MJ, DRUMMOND MS. Derivation of some modern arc magmas by melting of young subducted lithosphere[J]. *Nature*, 1990, 347(6294): 662-665.
- DOSTAL J, CHATTERJEE AK. Contrasting behaviour of Nb/Ta and Zr/Hf ratios in a peraluminous granitic pluton Nova Scotia, Canada[J]. *Chem. Geol.*, 2000, 163(1-4): 207-218.
- ERDMAN M. E., LEE Cintya. Oceanic- and continental-type metamorphic terranes: Occurrence and exhumation mechanisms [J]. *Earth-Science Reviews*, 2014, 139: 33-46.
- ERNST W. G. Subduction, ultrahigh-pressure metamorphism, and regurgitation of buoyant crustal slices — implications for arcs and continental growth [J]. *Physics of the Earth and Planetary Interiors*, 2001, 127(1-4): 253-275.
- ERNST W. G., LIOU Juhn. Contrasting plate-tectonic styles of the Qinling-Dabie-Sulu and Franciscan metamorphic belts [J]. *Geology*, 1995, 23(4): 353-356.
- FROST BR, BARNES CG, COLLINS WJ. A Geochemical classification for granitic rocks[J]. *Journal of Petrology*, 2001, 42: 2033-2048.
- GEHRELS GE, YIN An, WANG Xiaofeng. Magmatic history of the northeastern Tibetan Plateau[J/OL]. *Journal of Geophysical Research*, 2003, 108 (B9): doi: 10.1029/2002JB001876.
- GUO Jincheng, XU Xuming, CHEN Haiyan, et al. U-pb age of zircon from ultramafic rocks in Changshagou[A]. *Altyn and Its Geological Significance (in Chinese) [C]*, 2014.
- HARRIS NBW, INGER S. Trace element modelling of pelite-derived granites[J]. *Contributions to Mineralogy and Petrology*, 1992, 110 (1): 46-56.
- HE Zhenyu, ZHANG Zeming, ZONG Keqing, et al. Neoproterozoic granulites from the northeastern margin of the Tarim Craton: Petrology, zircon U-Pb ages and implications for the Rodinia assembly [J]. *Precambrian Res.*, 2012, 212-213: 21-33.
- HU Yunxu, XIAO Peixi, GAO Xiaofeng, et al. Regional stratigraphic division and establishment of stratigraphic time frame in the western section of east Kunlun - Altyn region[J]. *Northwestern Geology*. 2010, 43(4): 152-158(in Chinese)
- INGER, S., HARRIS, N. Geochemical constraints on leucogranite magmatism in the Langtang Valley, Nepal Himalaya[J]. *Journal of Petrology*, 1993, 34: 345-368.
- TARNEY, J. Geochemistry of Archaean high-grade gneisses, with implications as to the origin and evolution of the Precambrian crust[A]. In: WINDLEY, B. F. (ed) *The Early History of the Earth*. Wiley, London[C], 1976, 405-418.
- JOHANNES W, HOLTZ F. Petrogenesis and Experimental Petrology of Granitic Rocks[J]. *Minerals and Rocks*, Springer-Verlag, Berlin, 1996, 221-335.
- LIOU Juhn, ERNST W. G., SONG Shuguang, et al. Tectonics and HP-UHP metamorphism of northern Tibet- Preface [J]. *Journal of Asian Earth Sciences*, 2009b, 35(3-4): 191-198.
- LIOU Juhn, ERNST W. G., ZHANG Ruyuan, et al. Ultrahigh-pressure minerals and metamorphic terranes - The view from China [J]. *Journal of Asian Earth Sciences*, 2009a, 35(3-4): 199-231.
- LIOU Juhn, ZHANG Ruyuan, ERNST W. G. et al. High-pressure minerals from deeply subducted metamorphic rocks[J]. In PAUL L. Ribbe (ed.) *Mineral Society of America, Reviews in Mineralogy*, 1998, 37: 33-138.
- LIU Liang, SUN Yong, XIAO Peixi, et al. Discovery of ultrahigh-pressure magnesite-bearing garnet Iherzolite (> 3.8 GPa) in the Altyn Tagh, Northwest China[J]. *Chinese Science Bulletin*, 2002, 47(11): 881-886.
- LIU Liang, SUN Yong, LUO Jinhai, et al. Ultra-high pressure metamorphism of granitic gneiss in the Yinggelisayi area, Altun Mountains, NW China[J]. *Science in China (Series D)*, 2004, 47(4): 338-346.
- LIU Liang, CHEN Danling, ZHANG Anda, et al. Ultra-high pressure (>7GPa) gneissic K-feldspar (-bearing) garnet clinopyroxenite in the Altyn Tagh, NW China: Evidence from clinopyroxene exsolution in garnet[J].

- Science in China (Series D), 2005, 48(7): 1000-1010.
- LIU Liang, ZHANG Junfeng, GREEN II HW, et al. Evidence of former stishovite in metamorphosed sediments; Exhumation from > 350km [J]. Earth and Planetary Science Letters, 2007, 263(3-4): 180-191.
- LIU Liang, WANG Chao, CHEN Danling, et al. Petrology and geochronology of HP-UHP rocks from the south Altyn Tagh, northwestern China [J]. Journal of Asian Earth Sciences, 2009, 35(3-4): 232-244.
- LIU L, liang YANG Jiayi, CHEN Danling, et al. Progress and controversy in the study of HP-UHP metamorphic terranes in the West and Middle Central China orogen [J]. Journal of Earth Science, 2010, 21:(5), 581-597.
- LIU Liang, WANG Chao, CAO Yuting, et al. Geochronology of multi-stage metamorphic events; Constraints on episodic zircon growth from the UHP eclogite in the South Altyn, NW China [J]. Lithos, 2012, 136-139: 10-26.
- LONG, Xiaoping, YUAN Chao, SUN Min, et al. Reworking of the Tarim Craton by underplating of mantle plume-derived magmas: evidence from Neoproterozoic adakitic rocks and I-type granites in the Kuluketage area, NW China [J]. Precambrian Research, 2011, 187: 1-14.
- LONG, Xiaoping, SUN Min, YUAN Chao, et al. Zircon REE patterns and geochemical characteristics of Paleoproterozoic anatectic granite in the northern Tarim Craton, NW China: implications for the reconstruction of the Columbia supercontinent [J]. Precambrian Research, 2012, 222-223, 474-487.
- LU Songnian, LI Huaikun, YU Haifeng, et al. Neoproterozoic Orogeny in Northwestern China [J]. Gondwana Research, 1999, 2(4): 610-611.
- LU Songnian, LI Huaikun, ZHANG Chuanlin, et al. Geological and geochronological evidence for the Precambrian evolution of the Tarim Craton and surrounding continental fragments [J]. Precambrian Research, 2008, 160 (2008): 94-107.
- MA Xuxuan, SHU Liangshu, SANTOSH M, et al. Detrital zircon U-Pb geochronology and Hf isotope data from Central Tianshan suggesting a link with the Tarim Block; implications on Proterozoic supercontinent history [J]. Precambrian Research, 2012, 206-207, 1-16
- MANIAR PD, PICCOLI PM. Tectonic discrimination of granitoids [J]. Geological Society of America Bulletin, 1989, 101(5): 635-643.
- NESBITT HW, YOUNG G. Early Proterozoic climates and plate motions inferred from major element chemistry of lutites [J]. Nature 1982, 299(5885): 715-717.
- PEARCE JA, HARRIS NBW, ANDREW GT. Trace element discrimination diagrams for the tectonic interpretation of granitic rocks. Journal of Petrology, 1984, 25(4): 959-983.
- RAPP RP, WATSON EB. Dehydration Melting of Metabasalt at 8-32 kbar: Implications for Continental Growth and Crust-Mantle Recycling [J]. Journal of Petrology, 1995, 36(4): 891-931.
- RAPP RP, WATSON EB, MILLER CF. Partial melting of amphibolite/eclogite and the origin of Archaean trondhjemites and Tonalities [J]. Precambrian Research, 1991, 51(1-4): 1-25.
- REINECKE T. Very-high-pressure metamorphism and uplift of coesite-bearing metasediments from the Zermatt-Saas zone, Western Alps [J]. European Journal of Mineralogy, 1991, 3(1): 7-18.
- RGXR. Regional Geology of Xingjiang Uygur Autonomous Region [M]. Geological Publishing House, Beijing (in Chinese), 1993.
- RICKWOOD PC. Boundary lines within petrologic diagrams which use oxides of major and minor elements [J]. Lithos, 1989, 22(4): 247-263.
- ROLLINSON HR. Using geochemical data; evaluation, presentation, interpretation [M]. Harlow, Essex, England; New York; Longman Scientific & Technical, 1993, 1-352.
- RUBATTO D, Gebauer D, FANNING M. Jurassic formation and Eocene subduction of the Zermatt-Saas-Fee ophiolites: implications for the geodynamic evolution of the Central and Western Alps [J]. Contributions to Mineralogy and Petrology, 1998, 132(3): 269-287.
- SEARLE M P, FRYER B J. Garnet, tourmaline and muscovite-bearing leucogranites, gneisses and migmatites of the Higher Himalayas from Zaskar, Kulu, Lahoul and Kashmir [J]. Geological Society, London, Special Publications, 1986, 19, 185-201.
- SMITH D. C. A review of the peculiar mineralogy of the

- “Norwegian coesite-eclogite province”, with crystal-chemical, petrological, geochemical and geodynamical notes and an extensive bibliography In SMITH D C (ed.) [M]. Eclogites and eclogite-facies rocks. Amsterdam; Elsevier, 1988, 1-126.
- SONG Shuguang, ZHANG Lifei., NIU Yaoling., et al. Geochronology of diamond-bearing zircons from garnet peridotite in the North Qaidam UHPM belt, Northern Tibetan Plateau: A record of complex histories from oceanic lithosphere subduction to continental collision [J]. Earth and Planetary Science Letters, 2005, 234(1-2): 99-118.
- SONG Shuguang, SU Li, LI Xianhua, et al. Grenville-age orogenesis in the Qaidam-Qilian block: The link between South China and Tarim [J]. Precambrian Research, 2012, 220-221: 9-22.
- SONG Shuguang., NIU Yaoling., SU Li., et al. Continental orogenesis from ocean subduction, continent collision/subduction, to orogen collapse, and orogen recycling: The example of the North Qaidam UHPM belt, NW China [J]. Earth-Science Reviews, 2014a, 129: 59-84.
- SUN SS, MCDonough WF. Chemical and isotopic systematics of oceanic basalts: Implications for mantle composition and processes [J]. Geological Society London Special Publications 1989, 42(1): 313-345.
- SYLVERSTER PJ. Post-collisional strongly peraluminous granites [J]. Lithos, 1998, 45(1-4): 29-44.
- TAYLOR SR and MCLENNAN SM. The continental crust: Its composition and evolution [M]. Blackwell Scientific Publications, Oxford, 1985, 1-312.
- WANG Chao, LIU Liang, YANG Wenqiang, et al. Provenance and ages of the Altyn Complex in Altyn Tagh: Implications for the Early Neoproterozoic evolution of northwestern China [J]. Precambrian Research, 2013, 230: 193-208.
- WANG Chao, LIU Liang, CHEN Dsanling, et al. Petrology, geochemistry, geochronology and metamorphic evolution of garnet peridotites from South Altyn UHP terrane, NW China: Records related to crustal slab subduction and exhumation history [M]. Ultrahigh-Pressure Metamorphism - 25 Years After The Discovery Of Coesite And Diamond, 2011, 541-577.
- WANG Chao, WANG Yonghe, LIU Liang, et al. The Palaeoproterozoic magmatic - metamorphic events and cover sediments of the Tiekelik Belt along the southwestern margin of the Tarim Craton, northwestern China [J]. Precambrian Research, 2014, 254: 210-225.
- WATSON EB, HARRISON TM. Zircon saturation revisited: Temperature and composition effects in a variety of crustal magma types [J]. Earth and Planetary Science Letters, 1983, 64(2): 295-304.
- WATSON, EB., HARRISON, TM. Response to Comments on “Zircon thermometer reveals minimum melting conditions on earliest Earth” [J]. Science, 2006, 311(5762): 779.
- WINTHER KT, NEWTON RC. Experimental melting of hydrous low-K tholeiite: Evidence on the origin of Archean cratons [J]. Bulletin of the Geological Society of Denmark, 1991, 39: 213-228.
- YANG Wenqiang, LIU Liang, DING Haibo, et al. Geochemistry, geochronology and zircon Hf isotopes of the Dimunalike granite in South Altyn Tagh and its geological significance [J]. Acta Petrologica Sinica, 2012, 28(12): 4139-4150 (in Chinese with English abstract).
- YUAN Honglin, GAO Shan, LIU Xiaoming, et al. Accurate U-Pb age and trace element determinations of zircon by laser ablation-inductively coupled plasma-mass spectrometry [J]. Geostandards and Geoanalytical Research, 2004, 28(3): 353-370.
- ZHANG Jianxin, ZHANG Zeming, XU Zhiqin, et al. The Sm-Nd and U-Pb ages of eclogite [J]. Chinese Science Bulletin, 1999, 44: 1109-1112.
- ZHANG Jianxin, ZHANG Zeming, XU Zhiqin, et al. Petrology and geochronology of eclogite from the western segment of the Altyn Tagh, northwestern China [J]. Lithos, 2001, 56(2-3): 187-206.
- ZHANG Jianxin, YANG Jingsui, XU Zhiqin, et al. Evidence for UHP metamorphism of eclogites from the Altun Mountains [J]. Chinese Science Bulletin, 2002, 47(3): 231-234.
- ZHANG Anda, LIU Liang, SUN Yong, et al. SHRIMP U-Pb zircon ages for the UHP metamorphosed granitoid gneiss in Altyn Tagh and their geological significance [J]. Chinese Science Bulletin, 2004, 49(23): 2527-2532.
- ZHANG Jianxin, MATTINSON CG, MENG Fancong, et

- al. An Early Palaeozoic HP/HT granulite-garnet peridotite association in the south Altyn Tagh, NW China: P-T history and U-Pb geochronology[J]. *Journal of Metamorphic Geology*, 2005, 23(7):491-510.
- ZHANG Guibin, SONG Shuguang, ZHANG Lifei, et al. The subducted oceanic crust within continental-type UHP metamorphic belt in the North Qaidam, NW China: Evidence from petrology, geochemistry and geochronology[J]. *Lithos*, 2008a, 104(1-4): 99-118.
- ZHANG Jianxin, MATTINSON CG, YU Shengyao, et al. Combined rutile-zircon thermometry and U-Pb geochronology: New constraints on Early Paleozoic HP/UHT granulite in the south Altyn Tagh, north Tibet, China [J]. *Lithos*, 2014, 200-201:241-257.
- ZHANG Jianxin, MENG Fancong, YANG Jingsui. A new HP/LT metamorphic terrane in the northern Altyn Tagh, western China [J]. *International Geology Review*, 2005a, 47(4): 371-386
- ZHANG Jianxin, MENG Fancong, YU Shengyao, et al. 39Ar-40Ar geochronology of high- pressure/low- temperature blueschist and eclogite in the North Altyn Tagh and their tectonic implications [J]. *Geology in China*, 2007a, 34(4): 558-564 (in Chinese with English abstract)
- ZHANG Jianxin, LI Huaikun, MENG Fancong, et al. Polypphase tectonothermal events recorded in "metamorphic basement" from the Altyn Tagh, the southeastern margin of the Tarim basin, western China: Constraint from U-Pb zircon geochronology[J]. *Acta Petrologica Sinica*, 2011, 27(1):23-46.
- ZHANG Jianxin, YU Shengyao, MENG Fancong, et al. Paired high-pressure granulite and eclogite in collision orogens and their geodynamic implications [J]. *Acta Petrologica Sinica*, 2009, 25(9):2050-2066.
- ZHANG Qi, WANG Yan, LI Chengdong, et al. Granite classification on the basis of Sr and Yb contents and its implications[J]. *Acta Petrologica Sinica*, 2006, 22(9): 2249-2269( in Chinese with English abstract).
- ZHANG Qi, JIN Weijun, LI Chengdong, et al. Revisiting the new classification of granitic rocks based on whole-rock Sr and Yb contents: Index[J]. *Acta Petrologica Sinica*, 2010, 26(4):985-1015(in Chinese with English abstract).
- ZHENG Yongfei, ZHAO Zifu, WU Yuanbao, et al. Zircon U-Pb age, Hf and O isotope constraints on protolith origin of ultrahigh-pressure eclogite and gneiss in the Dabie orogen [J]. *Chemical Geology*, 2006, 231(1-2): 135-158.

## 余家山式基性-超基性岩同生铜镍矿床

成矿区带:龙门山一大巴山成矿带(Ⅲ-73)。

建造构造:汉南望江山基性岩体的西南边缘处,岩石类型主要有辉长岩、辉长辉绿岩、橄榄苏长辉长岩。岩石 m/f 变化于 0.9~3.6,平均为 1.4。望江山岩体黑云母的 Ar-Ar 法年龄 1120~1200 Ma(夏祖春等, 1987,汉南基性侵入岩矿物岩石研究报告。)

成矿时代:中元古代。

成矿组分:Cu, Ni, (Co)。

矿产地实例:(陕)西乡县余家山铜镍矿床,乔家山铜镍矿点。

简要特征:矿体主要赋存于辉长苏长岩,呈似层状、透镜状或扁豆状。矿石硫化物分布主要呈浸染状,次为块状。矿石金属矿物有磁黄铁矿、黄铁矿,次为紫硫镍铁矿,镍黄铁矿、针镍矿,含少量白铁矿、墨铜矿、方黄铜矿、铜蓝、蓝辉铜矿等;非金属矿物主要为辉石、橄榄石,次为斜长石、角闪石。矿石平均品位 Ni 0.35%, Cu 0.27%, Co 0.029%。

成因认识:中元古代晚期,在深部地幔热柱上涌和上部扬子地块覆盖保温的耦合条件下,地幔岩部分熔融的镁铁质岩浆,沿地块北缘薄弱地带侵入地壳,分异形成铜镍硫化物矿床(点)。